

# Heavy baryons in the relativized quark model with chromodynamics

Xin-Zhen Weng,<sup>1,\*</sup> Wei-Zhen Deng,<sup>2,†</sup> and Shi-Lin Zhu<sup>2,3,‡</sup>

<sup>1</sup>*School of Physics and Astronomy, Tel Aviv University, Tel Aviv 6997801, Israel*

<sup>2</sup>*School of Physics, Peking University, Beijing 100871, China*

<sup>3</sup>*Center of High Energy Physics, Peking University, Beijing 100871, China*

(Dated: October 1, 2024)

Following the work of Capstick and Isgur [Phys. Rev. D 34, 2809 (1986)], we systematically study the mass spectrum of the heavy baryons in the relativized quark potential model with chromodynamics. Besides the original Godfrey-Isgur (GI) model, we also adopt a modified GI model which replaces the linear confinement by a screened one. The two models give similar results in our work. All heavy baryons observed so far can be explained as three-quark states. In particular, we identify the  $\Omega_c(3000)/\Omega_b(6316)$ ,  $\Omega_c(3050)/\Omega_b(6330)$ ,  $\Omega_c(3065)/\Omega_b(6340)$ , and  $\Omega_c(3090)/\Omega_b(6350)$  states as the  $p_\lambda$  excitations with quantum numbers  $1/2^-$ ,  $3/2^-$ ,  $3/2^-$ , and  $5/2^-$ . The  $\Omega_c(3120)$  is a  $3/2^-$  state with the  $p_\rho$  excitation, whose bottom partner is predicted to be  $\Omega_b(6446/6457, 3/2^-)$ . The higher state  $\Omega_c(3188)$  is the  $2s_\lambda$  excitation with quantum numbers  $1/2^+$ , and  $\Omega_c(3327)$  is a  $d_\lambda$  excitation with quantum numbers  $3/2^+$  or  $5/2^+$ .

## I. INTRODUCTION

In the past few decades, we have seen large experimental progress in searching for the heavy baryons. Lots of charmed baryons were observed in the last few years. In 2017, the LHCb collaboration observed five narrow states in the  $\Xi_c^+ K^-$  mass spectrum:  $\Omega_c(3000)^0$ ,  $\Omega_c(3050)^0$ ,  $\Omega_c(3066)^0$ ,  $\Omega_c(3090)^0$ , and  $\Omega_c(3119)^0$  [1], where the first four of them were confirmed by the Belle collaboration [2]. Later LHCb observed  $\Lambda_c(2860)^+$  with quantum numbers  $J^P = 3/2^+$  in the  $D^0 p$  channel [3]. In 2020, LHCb further studied the  $\Lambda_c^+ K^-$  mass spectrum and observed  $\Xi_c(2923)^0$ ,  $\Xi_c(2939)^0$  and  $\Xi_c(2965)^0$  [4], where the first two are new states. In 2022, the Belle collaboration observed  $\Lambda_c(2910)^+$  decaying into  $\Sigma_c \pi$  [5]. Recently, the LHCb collaboration observed two new states  $\Omega_c(3185)^0$  and  $\Omega_c(3227)^0$  in the  $\Xi_c^+ K^-$  decay modes [6]. In addition, many bottom baryons were also found in experiments. In 2018, the LHCb collaboration reported the observation of  $\Sigma_b(6097)^\pm$  in the  $\Lambda_b^0 \pi^\pm$  final states [7]. The same year, they found the  $\Xi_b(6227)^-$  as a peak in both the  $\Lambda_b^0 K^-$  and  $\Xi_b^0 \pi^-$  invariant mass spectra [8]. The isospin partner  $\Xi_b(6227)^0$  was soon found [9]. In 2019, the LHCb collaboration observed the  $\Lambda_b(6146)^0$  and  $\Lambda_b(6152)^0$  in the  $\Lambda_b^0 \pi^+ \pi^-$  channel [10]. Another state  $\Lambda_b(6072)^0$  was also found in the same channel by the CMS collaboration [11]. In 2020, the LHCb collaboration observed four narrow peak,  $\Omega_b(6316)^-$ ,  $\Omega_b(6330)^-$ ,  $\Omega_b(6340)^-$ , and  $\Omega_b(6350)^-$ , in the  $\Xi_b^0 K^-$  channel [12]. Later in 2021, the CMS collaboration found  $\Xi_b(6100)^-$  in the  $\Xi_b^- \pi^+ \pi^-$  channel [13]. Recently, the LHCb collaboration confirmed the existence of  $\Xi_b(6227)^0$  and observed another state  $\Xi_b(6333)^0$  [14]. To date, there are 42 singly-charmed and 25 singly-bottomed baryons col-

lected in PDG [15], plus 3 singly-charmed and 1 singly-bottomed baryons observed more recently.

Inspired by the experimental progress, physicists used various methods to study heavy baryons, such as the quark models [16–41], lattice QCD [42–48], QCD sum rules [49–55], heavy quark effective theory (HQET) [56], and the Regge phenomenology [57–59]. For extra references, see recent review Refs. [60–65].

A well-known quark potential model is the relativized quark model proposed by Godfrey and Isgur (GI) in 1985 [66], which was used to investigate the meson systems extensively [66–72]. In 1986, Capstick and Isgur extended this model to study the baryon systems [73]. Due to the lack of experimental data of heavy baryons, their work mainly focus on the light baryons and  $nnQ$  baryons [Here, we assume SU(2) isospin symmetry and denote  $n = \{u, d\}$ ]. In Refs. [74, 75], Lü *et al.* used this model, together with the diquark approximation, to study the  $\Lambda_c$  and doubly heavy baryons. Recently, Yu *et al.* studied the singly and doubly heavy baryons within this model [76–80]. However, they assumed  $\{l_\rho l_\lambda L S j\} I J^P$  ( $j = l_\rho + S$ ) to be good quantum numbers, while the Hamiltonian only ascertains that the  $I J^P$  are good quantum numbers. Furthermore, they ignored the  $l_\rho \neq 0$  ( $l_\lambda \neq 0$ ) components for the singly (doubly) heavy baryons. In this series, we will investigate the spectra of heavy baryons in the GI model, without using these approximations.

When going to the higher excited states, the coupled-channel effects may be of importance. For instance, the physical  $D_{s_0}^*(2317)$  and  $D_{s_1}^*(2460)$  are the mixture of the  $c\bar{s}$  core and the  $D^{(*)}K$  component [81]. Another example would be the  $X(3872)$  of  $J^{PC} = 1^{++}$ . Its mass is about 80 MeV lower than the theoretical prediction in the GI [66] and similar quark potential models. Theoretical studies suggested that the coupled-channel effect with  $D\bar{D}^*$  is very important [82–85]. In the baryon sector, the  $\Lambda_c(2910)$  and  $\Lambda_c(2940)$  are argued to be conventional  $\Lambda_c$  excitations dressed with the  $D^*N$  channel [86, 87]. In Ref. [88], Li *et al.* found that the coupled-channel model

\* xinzhenweng@mail.tau.ac.il

† dwz@pku.edu.cn

‡ zhushl@pku.edu.cn

and the screened potential model have similar global features in describing the charmonium spectrum (below 4.0 GeV) since they approximately embody the same effect of the vacuum polarization of dynamical light quark pairs. Based on this observation, Song *et al.* implemented the GI model by replacing the linear confining potential  $br$  by a screened one  $V^{\text{scr}} = b(1 - e^{-\mu r})/\mu$  to reflect the coupled-channel effect [89]. They found that the modified GI (MGI) model is more suitable to describe the experimental data, especially the higher excited mesons [89–92].

In this work, we use the two relativized quark models, both GI and MGI models, to study the mass spectra of the singly heavy baryons. In Sec II, we briefly introduce the models. Then we present the numerical results and discussions in Sec. III. Finally, we conclude in Sec. IV.

## II. THE RELATIVIZED QUARK MODEL

### A. Godfrey-Isgur (GI) model

In the relativized quark model, the Hamiltonian of a baryon reads [66, 73]

$$H = H_0 + V_{\text{OGE}} + V_{\text{conf}}, \quad (1)$$

where

$$H_0 = \sum_{i=1}^3 (\mathbf{p}_i^2 + m_i^2)^{1/2} \quad (2)$$

is the relativistic kinetic energy, in which  $m_i$  and  $\mathbf{p}_i$  are the  $i$ th quark's mass and momentum.  $V_{\text{OGE}}$  is a one-gluon-exchange (OGE) potential, and  $V_{\text{conf}}$  consists of a string potential and a spin-orbit term arising via Thomas precession.

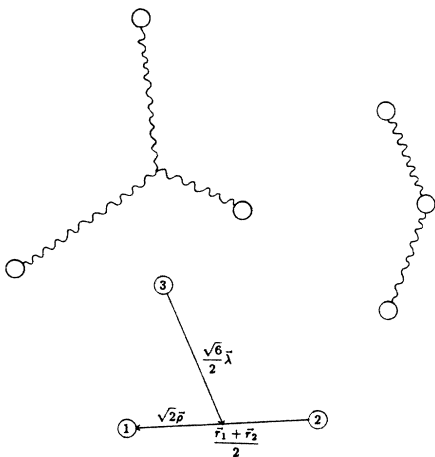


FIG. 1. The string confinement and the relative coordinates  $\rho$  and  $\lambda$  [73].

In the nonrelativistic limit, the potentials go to the

usual Breit-Fermi interaction

$$V_{\text{OGE}} \rightarrow \sum_{i<j} \left( V_{ij}^{\text{Coul}} + V_{ij}^{\text{hyp}} + V_{ij}^{\text{so}(v)} \right), \quad (3)$$

and

$$V_{\text{conf}} \rightarrow V_{\text{string}} + \sum_{i<j} V_{ij}^{\text{so}(v)}. \quad (4)$$

Here,  $V_{ij}^{\text{Coul}}$  is the spin-independent Coulomb-type interaction;  $V_{ij}^{\text{hyp}}$  is the color-hyperfine interaction which consists of the contact and tensor interaction;  $V_{ij}^{\text{so}(v)} + V_{ij}^{\text{so}(v)}$  is the spin-orbit interaction, and  $V_{\text{string}}$  is the three-body  $Y$ -shape confinement interaction (see Fig. 1)

$$V_{\text{string}} = C_{qqq} + b \sum_{i=1}^3 |\mathbf{r}_i - \mathbf{r}_{\text{junction}}|. \quad (5)$$

The  $V_{\text{string}}$  interaction can be broken into an effective two-body piece and a three-body piece

$$V_{\text{string}} = C_{qqq} + fb \sum_{i<j} r_{ij} + V_{3b} \quad (6)$$

where

$$V_{3b} = b \left( \sum_{i=1}^3 |\mathbf{r}_i - \mathbf{r}_{\text{junction}}| - f \sum_{i<j} r_{ij} \right) \quad (7)$$

with  $f = 0.5493$  [73, 93, 94] chosen to minimize the size of the expectation value of  $V_{3b}$ . Then the  $V_{3b}$  can be treated perturbatively. Note that the contribution of  $V_{3b}$  is *always small* [73] and we will not consider it in the present work for simplification.

As pointed out in Refs. [66, 73], the Breit-Fermi interaction should be modified for many reasons: (a) the proceeding potentials are constructed by reproducing the *on-shell*  $qq$  scattering, which will be modified by the off-shell properties of quark; (b) the constituent quarks are not pointlike, but rather will have a graininess appropriate to some finite scale  $\mu$ ; (c) the higher Fock space such as  $|qqqg\rangle$  is not considered in the present work, which will introduce additional momentum-dependence in the potential. To incorporate these effects, Godfrey and Isgur further built a semiquantitative *model* [66]. Firstly, by introducing the smearing function

$$\rho_{ij}(\mathbf{r} - \mathbf{r}') = \frac{\sigma_{ij}^3}{\pi^{3/2}} e^{-\sigma_{ij}^2 (\mathbf{r} - \mathbf{r}')^2}, \quad (8)$$

the potentials  $V_{ij}^{\text{OGE}}$  and  $V_{ij}^{\text{conf}}$  are smeared to  $\tilde{V}_{ij}^{\text{OGE}}$  and  $\tilde{V}_{ij}^{\text{conf}}$  via

$$\tilde{V}_{ij}(r) = \int d^3r' \rho_{ij}(\mathbf{r} - \mathbf{r}') V_{ij}(r'), \quad (9)$$

with the prescription

$$\sigma_{ij}^2 = \frac{\sigma_0^2}{2} \left\{ 1 + \left[ \frac{4m_i m_j}{(m_i + m_j)^2} \right]^4 \right\} + s^2 \left( \frac{2m_i m_j}{m_i + m_j} \right)^2, \quad (10)$$

where  $\sigma_0$  and  $s$  are free parameters. Secondly, through the introduction of the momentum-dependent factors, the Coulomb term is modified according to

$$\tilde{V}_{ij}^{\text{Coul}} \rightarrow (\beta_{ij})^{1/2+\epsilon_{\text{Coul}}} \tilde{V}_{ij}^{\text{Coul}} (\beta_{ij})^{1/2+\epsilon_{\text{Coul}}}, \quad (11)$$

and the contact, tensor, vector spin-orbit, and scalar spin-orbit potentials are modified according to

$$\tilde{V}_{ij}^{\alpha} \rightarrow \left( \delta_{ij}^{[ij]} \right)^{1/2+\epsilon_{\alpha}} \tilde{V}_{ij}^{\alpha} \left( \delta_{ij}^{[ij]} \right)^{1/2+\epsilon_{\alpha}} \quad (12)$$

where  $\epsilon_{\alpha}$  corresponds to the contact (cont), tensor (tens), vector spin-orbit [so(v)], and scalar spin-orbit [so(s)]. The momentum-dependent factors are

$$\beta_{ij} = 1 + \frac{p_{ij}^2}{(p_{ij}^2 + m_i^2)^{1/2}(p_{ij}^2 + m_j^2)^{1/2}} \quad (13)$$

and

$$\delta_{ij}^{[i'j']} = \frac{m_i m_j}{(p_{i'j'}^2 + m_i^2)^{1/2}(p_{i'j'}^2 + m_j^2)^{1/2}}, \quad (14)$$

where  $p_{ij}$  is the magnitude of the momentum of either of the quarks in the  $ij$  center-of-mass frame.

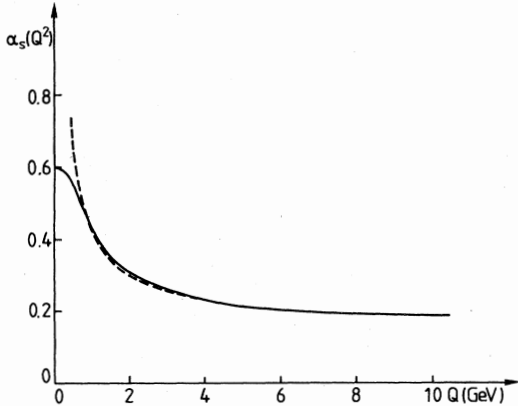


FIG. 2. The leading order QCD formula (15) for the effective coupling constant with  $\Lambda_{\text{QCD}} = 200$  MeV and the fit  $\alpha_s(Q^2) = 0.25e^{-Q^2} + 0.15e^{-Q^2/10} + 0.20e^{-Q^2/1000}$  ( $Q^2$  in  $\text{GeV}^2$ ) [66, 73].

The last piece of the model is the QCD coupling constant  $\alpha_s$ . With  $N_f$  flavors of quark with masses below

$Q^2$ , the lowest-order coupling constant reads

$$\alpha_s(Q^2) = \frac{12\pi}{33 - 2N_f \ln(Q^2/\Lambda_{\text{QCD}}^2)}. \quad (15)$$

The  $\alpha_s(Q^2)$  is small for large  $Q^2$  but diverges as  $Q^2$  approach  $\Lambda_{\text{QCD}} \approx 200$  MeV, which indicates the confinement. Since we are interested in the soft regime, we cannot avoid this divergence; rather we assume that  $\alpha_s$  saturates at some value  $\alpha_s^{\text{critical}}$  for low  $Q^2$  as confinement emerges. For convenience, the coupling constant  $\alpha_s$  is parametrized as

$$\alpha_s(Q^2) = \sum_k \alpha_k e^{-Q^2/4\gamma_k^2}, \quad (16)$$

where

$$\alpha_s^{\text{critical}} = \sum_k \alpha_k \quad (17)$$

is a free parameter. Fitting the QCD curve [Eq. (15), see Fig. 2] gives [66]

$$\alpha_s(Q^2) = 0.25e^{-Q^2} + 0.15e^{-Q^2/10} + 0.20e^{-Q^2/1000} \quad (18)$$

with  $Q^2$  in  $\text{GeV}^2$ .

Now we can finally present the effective potentials [73]. The smeared OGE propagator is

$$\tilde{G}(r_{ij}) = - \sum_k \frac{2\alpha_k}{3r_{ij}} \cdot \text{Erf}(\tau_{kij} r_{ij}) \quad (19)$$

where  $\text{Erf}(x)$  is the Gauss error function and

$$\frac{1}{\tau_{kij}^2} = \frac{1}{\gamma_k^2} + \frac{1}{\sigma_{ij}^2}. \quad (20)$$

All of the OGE potential can be expressed in terms of  $\tilde{G}(r_{ij})$ . More precisely, the OGE potentials

$$\tilde{V}_{\text{OGE}} = \sum_{i < j} \tilde{V}_{ij}^{\text{OGE}} \quad (21)$$

with

$$\tilde{V}_{ij}^{\text{OGE}} = \tilde{V}_{ij}^{\text{Coul}} + \tilde{V}_{ij}^{\text{hyp}} + \tilde{V}_{ij}^{\text{so}(v)} \quad (22)$$

where

$$\tilde{V}_{ij}^{\text{Coul}} = (\beta_{ij})^{1/2+\epsilon_{\text{Coul}}} \tilde{G}(r_{ij}) (\beta_{ij})^{1/2+\epsilon_{\text{Coul}}} \quad (23)$$

is the Coulomb-type interaction.

$$\tilde{V}_{ij}^{\text{hyp}} = \tilde{V}_{ij}^{\text{cont}} + \tilde{V}_{ij}^{\text{tens}} \quad (24)$$

is the hyperfine interaction with contact term

$$\tilde{V}_{ij}^{\text{cont}} = \left( \delta_{ij}^{[ij]} \right)^{1/2+\epsilon_{\text{cont}}} \frac{2\mathbf{S}_i \cdot \mathbf{S}_j}{3m_i m_j} \nabla_{r_{ij}}^2 \tilde{G}(r_{ij}) \left( \delta_{ij}^{[ij]} \right)^{1/2+\epsilon_{\text{cont}}} \quad (25)$$

and tensor term

$$\tilde{V}_{ij}^{\text{tens}} = \left(\delta_{ij}^{[ij]}\right)^{1/2+\epsilon_{\text{tens}}} \frac{1}{3m_i m_j} \left( \frac{3\mathbf{S}_i \cdot \mathbf{r}_{ij} \mathbf{S}_j \cdot \mathbf{r}_{ij}}{r_{ij}^2} - \mathbf{S}_i \cdot \mathbf{S}_j \right) \left( \frac{1}{r_{ij}} \frac{d\tilde{G}(r_{ij})}{dr_{ij}} - \frac{d^2\tilde{G}(r_{ij})}{dr_{ij}^2} \right) \left(\delta_{ij}^{[ij]}\right)^{1/2+\epsilon_{\text{tens}}}. \quad (26)$$

$$\begin{aligned} \tilde{V}_{ij}^{\text{so}(v)} = \frac{1}{r_{ij}} \frac{d\tilde{G}(r_{ij})}{dr_{ij}} \left[ \left(\delta_{ii}^{[ij]}\right)^{1/2+\epsilon_{\text{so}(v)}} \frac{\mathbf{r}_{ij} \times \mathbf{p}_i \cdot \mathbf{S}_i}{2m_i^2} \left(\delta_{ii}^{[ij]}\right)^{1/2+\epsilon_{\text{so}(v)}} - \left(\delta_{jj}^{[ij]}\right)^{1/2+\epsilon_{\text{so}(v)}} \frac{\mathbf{r}_{ij} \times \mathbf{p}_j \cdot \mathbf{S}_j}{2m_j^2} \left(\delta_{jj}^{[ij]}\right)^{1/2+\epsilon_{\text{so}(v)}} \right. \\ \left. - \left(\delta_{ij}^{[ij]}\right)^{1/2+\epsilon_{\text{so}(v)}} \frac{\mathbf{r}_{ij} \times \mathbf{p}_j \cdot \mathbf{S}_i - \mathbf{r}_{ij} \times \mathbf{p}_i \cdot \mathbf{S}_j}{m_i m_j} \left(\delta_{ij}^{[ij]}\right)^{1/2+\epsilon_{\text{so}(v)}} \right] \end{aligned} \quad (27)$$

is the spin-orbit interaction.

The confinement potential  $V_{\text{conf}}$  consists of a string potential and a spin-orbit term arising from Thomas precession

$$\tilde{V}_{\text{conf}} = C_{qqq} + \sum_{i<j} \tilde{V}_{ij}^{\text{string}} + \sum_{i<j} \tilde{V}_{ij}^{\text{so}(s)} \quad (28)$$

with

$$\tilde{V}_{ij}^{\text{string}} = f b r_{ij} \left[ \frac{e^{-\sigma_{ij}^2 r_{ij}^2}}{\sqrt{\pi} \sigma_{ij} r_{ij}} + \left( 1 + \frac{1}{2\sigma_{ij}^2 r_{ij}^2} \right) \text{Erf}(\sigma_{ij} r_{ij}) \right] \quad (29)$$

and

$$\tilde{V}_{ij}^{\text{so}(s)} = -\frac{1}{r_{ij}} \frac{\partial \tilde{V}_{ij}^{\text{string}}}{\partial r_{ij}} \left[ \left(\delta_{ii}^{[ij]}\right)^{1/2+\epsilon_{\text{so}(s)}} \frac{\mathbf{r}_{ij} \times \mathbf{p}_i \cdot \mathbf{S}_i}{2m_i^2} \left(\delta_{ii}^{[ij]}\right)^{1/2+\epsilon_{\text{so}(s)}} - \left(\delta_{jj}^{[ij]}\right)^{1/2+\epsilon_{\text{so}(s)}} \frac{\mathbf{r}_{ij} \times \mathbf{p}_j \cdot \mathbf{S}_j}{2m_j^2} \left(\delta_{jj}^{[ij]}\right)^{1/2+\epsilon_{\text{so}(s)}} \right] \quad (30)$$

where we have ignored the small perturbation term  $V_{3b}$  [Eq. (7)].

## B. Modified Godfrey-Isgur (MGI) model with the screening effect

In order to take into account the screening effect, Refs. [89, 90] proposed the following replacement for the linear confinement interaction

$$b r \rightarrow V^{\text{scr}}(r) = \frac{b(1 - e^{-\mu r})}{\mu}. \quad (31)$$

where  $V^{\text{scr}}(r)$  behaves like the linear confinement potential  $br$  at short distance and approaches constant  $b/\mu$  at long distance. After smearing, we have

$$\tilde{V}_{\text{conf}} \rightarrow \tilde{V}_{\text{conf}}^{\text{scr}} = C_{qqq} + \sum_{i<j} \tilde{V}_{ij}^{\text{scr}} + \sum_{i<j} \tilde{V}_{ij}^{\text{so}(\text{scr})} \quad (32)$$

where

$$\begin{aligned} \tilde{V}_{ij}^{\text{scr}} = \frac{fb}{\mu} \left\{ 1 - \frac{1}{2\sigma_{ij} r_{ij}} \left[ \left( \frac{\mu}{2\sigma_{ij}} + \sigma_{ij} r_{ij} \right) \exp\left( \frac{\mu^2}{4\sigma_{ij}^2} + \mu r_{ij} \right) \cdot \text{Erfc}\left( \frac{\mu}{2\sigma_{ij}} + \sigma_{ij} r_{ij} \right) \right. \right. \\ \left. \left. - \left( \frac{\mu}{2\sigma_{ij}} - \sigma_{ij} r_{ij} \right) \exp\left( \frac{\mu^2}{4\sigma_{ij}^2} - \mu r_{ij} \right) \cdot \text{Erfc}\left( \frac{\mu}{2\sigma_{ij}} - \sigma_{ij} r_{ij} \right) \right] \right\}, \end{aligned} \quad (33)$$

and

$$\tilde{V}_{ij}^{\text{so}(\text{scr})} = -\frac{1}{r_{ij}} \frac{\partial \tilde{V}_{ij}^{\text{scr}}}{\partial r_{ij}} \left[ \left(\delta_{ii}^{[ij]}\right)^{1/2+\epsilon_{\text{so}(s)}} \frac{\mathbf{r}_{ij} \times \mathbf{p}_i \cdot \mathbf{S}_i}{2m_i^2} \left(\delta_{ii}^{[ij]}\right)^{1/2+\epsilon_{\text{so}(s)}} - \left(\delta_{jj}^{[ij]}\right)^{1/2+\epsilon_{\text{so}(s)}} \frac{\mathbf{r}_{ij} \times \mathbf{p}_j \cdot \mathbf{S}_j}{2m_j^2} \left(\delta_{jj}^{[ij]}\right)^{1/2+\epsilon_{\text{so}(s)}} \right] \quad (34)$$

where  $\text{Erfc}(x)$  is the complementary error function.

## C. Baryon wave function

To investigate the mass spectra of the baryons, we need to construct the wave functions. The total wave function

is a direct product of the flavor, color, spin, and spatial

wave functions.

In this work, we ignore the isospin violation and abbreviate  $n = \{u, d\}$ . The flavor wave functions of heavy baryons can be easily written down directly. Note that for the  $nnQ$  systems we have  $\{nn\}Q$  for  $\Sigma_Q$  with isospin  $I = 1$  and  $[nn]Q$  for  $\Lambda_Q$  with  $I = 0$ , where we use the brace  $\{\dots\}$  to symmetrize the quark flavors and the bracket  $[\dots]$  to antisymmetrize the flavors.

The baryons should be color-singlet, thus we have only one totally antisymmetric color wave function

$$\varphi^c = |(q_1 q_2)^3 c q_3\rangle^{1c}. \quad (35)$$

where the superscripts are color representations.

Next we consider the spin wave functions. The total spin of the baryons can be either of  $1/2$  or  $3/2$ . A complete set of the spin wave functions are listed as follows

$$\begin{cases} \chi_1^s = |(q_1 q_2)_1 q_3\rangle_{3/2}, \\ \chi_2^s = |(q_1 q_2)_1 q_3\rangle_{1/2}, \\ \chi_3^s = |(q_1 q_2)_0 q_3\rangle_{1/2}, \end{cases} \quad (36)$$

where the subscripts are spins  $\{S_{12}, S\}$ . The third component  $M_S$  is not shown for simplicity.

Finally for spatial wave functions we adopt the harmonic-oscillator wave function

$$\begin{aligned} \Psi_{LM_L n_\rho l_\rho n_\lambda l_\lambda}(\boldsymbol{\rho}, \boldsymbol{\lambda}) &= \sum_{m_{l_\rho} m_{l_\lambda}} \langle l_\rho m_{l_\rho}; l_\lambda m_{l_\lambda} | LM_L \rangle \\ &\times \psi_{n_\rho l_\rho m_{l_\rho}}(\boldsymbol{\alpha}, \boldsymbol{\rho}) \psi_{n_\lambda l_\lambda m_{l_\lambda}}(\boldsymbol{\alpha}, \boldsymbol{\lambda}) \end{aligned} \quad (37)$$

in the two relative coordinates (see Fig. 1)

$$\begin{cases} \boldsymbol{\rho} = \frac{\mathbf{r}_1 - \mathbf{r}_2}{\sqrt{2}}, \\ \boldsymbol{\lambda} = \frac{\mathbf{r}_1 + \mathbf{r}_2 - 2\mathbf{r}_3}{\sqrt{6}}, \end{cases} \quad (38)$$

and  $\psi_{nlm}(\boldsymbol{\alpha}, \boldsymbol{r})$  is the harmonic oscillator wave function with variational parameter  $\alpha$ .

We then expand the wave function of quantum numbers  $J^P$  in states of the form

$$\begin{aligned} |\alpha\rangle &= \chi^f \varphi^c \sum_{M_L M_S} \langle LM_L; SM_S | JM \rangle \\ &\times \Psi_{LM_L n_\rho l_\rho n_\lambda l_\lambda} \chi_{SM_S}^s, \end{aligned} \quad (39)$$

where  $P = (-1)^{l_\rho + l_\lambda}$ . Note that there are infinite number of bases for any quantum numbers  $IJ^P$ . We truncate the bases by  $N \leq 10$  with  $N = 2(n_\rho + n_\lambda) + l_\rho + l_\lambda$ . Diagonalizing the Hamiltonian in these bases and minimizing each eigenvalues by varying  $\alpha$ , we obtain the mass spectra of the heavy baryons. More details can be found in Ref. [73].

TABLE I. The parameters of the relativized quark potential model. Note that we ignore isospin violation.

Parameters	GI85 [66]	CI86 [73]	This work	
			GI	MGI
Masses (MeV)				
$m_n$	220	220	247	244
$m_s$	419	419	455	452
$m_c$	1628	1628	1652	1644
$m_b$	4977	4977	5000	4991
Potentials				
$b$ (GeV <sup>2</sup> )	0.18	0.15	0.14	0.17
$\alpha_s^{\text{critical}}$	0.60	Same	Same	Same
$\Lambda_{\text{QCD}}$ (MeV)	220	Same	Same	Same
$C_{q\bar{q}}$ (MeV)	$\frac{4}{3}(-253) = -340$	—	—	—
$C_{qqq}$ (MeV)	—	-615	-547	-656
$\mu$ (MeV)	—	—	—	0.06
Relativistic effects				
$\sigma_0$ (GeV)	1.80	1.80	1.60	1.60
$s$	1.55	1.55	1.75	1.67
$\epsilon_{\text{Coul}}$	—	0	+0.060	+0.071
$\epsilon_{\text{cont}}$	-0.168	-0.168	-0.179	-0.173
$\epsilon_{\text{tens}}$	+0.025	-0.168	-0.015	-0.125
$\epsilon_{\text{so}(v)}$	-0.035	0	-0.220	-0.237
$\epsilon_{\text{so}(s)}$	+0.055	+0.300	+0.039	-0.062

### III. NUMERICAL RESULTS

#### A. Parameters

The GI model is successful in studying the mesons and baryons. In 1985, Godfrey and Isgur fitted the parameters for mesons [66]. Later Capstick and Isgur refitted the parameters for the baryons [73]. The concrete values of these parameters are collected in Table I. After their works, lots of heavy baryons had been observed in experiments [15]. To appreciate the experimental progress in the past three decades, we perform the  $\chi^2$  fits to obtain the 13/14 parameters of the GI/MGI models. The  $\chi^2$  is defined as

$$\chi^2 = \sum_i \frac{(m_i^{\text{exp.}} - m_i^{\text{th.}})^2}{\sigma_i^2}, \quad (40)$$

where the  $m_i^{\text{exp.}}$  and  $m_i^{\text{th.}}$  are experimental and theoretical masses of the baryons. The baryons used for

TABLE II. Masses of light and singly-heavy baryons used for fitting parameters. All masses are in units of MeV.

State, $J^P$	CI86 [73]	This work		Exp. [15]	State, $J^P$	CI86 [73]	This work		Exp. [15]
		GI	MGI				GI	MGI	
$N\frac{1}{2}^+$	960	948	946	$938.9187544 \pm 0.0000003^a$	$\Delta\frac{3}{2}^+$	1230	1233	1232	$1232 \pm 2$
$\Lambda\frac{1}{2}^+$	1115	1122	1122	$1115.683 \pm 0.006$					
$\Sigma\frac{1}{2}^+$	1190	1179	1179	$1193.15 \pm 0.03$	$\Sigma\frac{3}{2}^+$	1370	1387	1388	$1384.6 \pm 0.4$
$\Xi\frac{1}{2}^+$	1305	1318	1318	$1318.28 \pm 0.11$	$\Xi\frac{3}{2}^+$	1505	1532	1535	$1533.4 \pm 0.3$
					$\Omega\frac{3}{2}^+$	1635	1668	1670	$1672.45 \pm 0.29$
$\Lambda_c\frac{1}{2}^+$	2265	2290	2288	$2286.46 \pm 0.14$	$\Lambda_c^*\frac{3}{2}^+$	<u>2910</u>	2870	2871	$2856.1_{-6.0}^{+2.3}$
$\Lambda_c^*\frac{1}{2}^-$	<u>2630</u> <sup>b</sup>	2594	2592	$2592.25 \pm 0.28$	$\Lambda_c^*\frac{3}{2}^-$	<u>2640</u>	2624	2627	$2628.11 \pm 0.19$
$\Sigma_c\frac{1}{2}^+$	2440	2439	2437	$2453.45 \pm 0.10$	$\Sigma_c\frac{3}{2}^+$	<u>2495</u>	2519	2518	$2518.1 \pm 0.3$
$\Xi_c\frac{1}{2}^+$	—	2476	2474	$2469.08 \pm 0.18$	$\Xi_c\frac{3}{2}^+$	—	2649	2649	$2645.63 \pm 0.20$
	—	2572	2571	$2578.5 \pm 0.4$					
$\Xi_c^*\frac{1}{2}^-$	—	2787	2793	$2792.9 \pm 0.4$	$\Xi_c^*\frac{3}{2}^-$	—	2814	2818	$2818.15 \pm 0.20$
$\Omega_c\frac{1}{2}^+$	—	2695	2692	$2695.2 \pm 1.7$	$\Omega_c\frac{3}{2}^+$	—	2769	2768	$2765.9 \pm 2.0$
$\Lambda_b\frac{1}{2}^+$	<u>5585</u>	5625	5623	$5619.60 \pm 0.17$					
$\Lambda_b^*\frac{1}{2}^-$	<u>5912</u>	5894	5896	$5912.19 \pm 0.17$	$\Lambda_b^*\frac{3}{2}^-$	<u>5920</u>	5906	5908	$5920.09 \pm 0.17$
$\Sigma_b\frac{1}{2}^+$	<u>5795</u>	5809	5809	$5813.10 \pm 0.18$	$\Sigma_b\frac{3}{2}^+$	<u>5805</u>	5838	5838	$5832.53 \pm 0.20$
$\Xi_b\frac{1}{2}^+$	—	5805	5803	$5794.5 \pm 0.4$	$\Xi_b\frac{3}{2}^+$	—	5963	5964	$5953.8 \pm 0.3$
	—	5935	5934	$5935.02 \pm 0.05$					
$\Omega_b\frac{1}{2}^+$	—	6049	6047	$6045.2 \pm 1.2$					

<sup>a</sup> The baryon masses are taken by their isospin averages.

<sup>b</sup> Most heavy baryons are observed after the publication of Ref. [73]. These states are indicated by an underline.

fits include 24 ground states and 6 excited states (see Table II). The  $\sigma_i$  is usually chosen to be the uncertainty of the experimental mass  $\Delta m_i^{\text{exp.}}$ . However, the  $\Delta m_N^{\text{exp.}} \sim 10^{-7}$  MeV is too small compares to the uncertainties of other baryons, which will deteriorate the fits. Thus we choose  $\sigma_i$  to be a constant

$$\sigma_i = k \text{ MeV}. \quad (41)$$

The results are independent of the concrete value of  $k$ . Our fits give  $\chi^2 = \{1776, 1558\}/k^2$  for the GI and MGI models, respectively. The parameters obtained are listed in Table I. The comparison of the fitted masses with experimental data is listed in Table II. With parameters obtained, we can calculate the heavy baryon masses. The spectroscopic results are given in Tables III–VI and Figs. 3–10. Within uncertainty of the quark model, the GI and MGI models give similar results.

## B. The $\Sigma_Q$ and $\Lambda_Q$ baryons

The  $\Sigma_Q$  and  $\Lambda_Q$  baryon masses are listed in Tables III–IV. Their relative positions are plotted in Figs. 3–6.

First we consider the  $\Sigma_c$  baryons. From Fig. 3, we can clearly see that the low-lying states form band structures. The lowest band consists of the ground states of spin  $1/2^+$  and  $3/2^+$ . The next band consists of seven negative parity states dominated by  $P$ -wave excitation components. Among them, the  $1/2^-$  and  $3/2^-$  states further form a two semi-band structure. The lower two states are dominated by  $p_\lambda$  modes, while the higher ones are dominated by  $p_\rho$  excitations. In 2004, the Belle Collaboration observed the  $\Sigma_c(2800)$  state in the  $\Lambda_c\pi$  channel [95]. Its quantum numbers are not determined yet [15]. Our calculation suggests that it is most likely a  $3/2^-$  state dominated by the  $p_\lambda$  excitation. The third band is dominated by the  $N = 2$  excitation (For convenience, we use the oscillator band to label the quark model states. When we refer to a state within  $N = 2$  band, we are implying that *most* part of its wave functions belong to the  $N = 2$  band of oscillator). More precisely, this band consists of  $2s_\rho$ ,

$2s_\lambda$ ,  $d_\rho$ ,  $d_\lambda$  and  $[p_\rho p_\lambda]_L$  excitations. We again find that the excitation over  $\lambda$  mode is easier than over  $\rho$  mode. Taking  $1/2^+$  states as an example, the  $\Sigma_c(2925/2923)$  and  $\Sigma_c(3025/3032)$  are dominated by the  $2s_\lambda$  and  $d_\lambda$  modes, the  $\Sigma_c(3096/3112)$  and  $\Sigma_c(3119/3118)$  are dominated by  $d_\rho$  and  $2s_\rho$  modes, while the  $\Sigma_c(3025/3040)$  and  $\Sigma_c(3165/3180)$  are both dominated by the  $[p_\rho p_\lambda]_L$  mode. We also calculate the heavier states which include higher excitations. They are more packed with each other. A more detailed study of their decay properties is needed.

The  $\Sigma_b$  baryon spectrum is similar. A main difference is that the splitting between the excitations over  $\lambda$  and  $\rho$  is larger. For the  $1/2^-$  states in the  $N = 1$  band, the  $p_\lambda$ - $p_\rho$  is about 110 MeV for the  $\Sigma_b$  states and 80 MeV for the  $\Sigma_c$  states. The  $3/2^-$  states are similar. Another consequence is that the  $N = 2$  band begins to overlap with the  $N \leq 2$  bands. Experimentally, there is one  $\Sigma_b$  excited state observed by the LHCb Collaboration, namely the  $\Sigma_b(6097)$  [7]. Our calculation suggests that it is a  $1/2^-$  or  $3/2^-$  state dominated by the  $p_\lambda$  excitation.

Next we turn to the  $\Lambda_Q$  baryons. From Figs. 5–6, we see that our calculated results fit quite well with the experimental observations. In Sec. III A, we used the lowest  $1/2^\pm$  and  $3/2^\pm$   $\Lambda_Q$  states for parameter fits. There remain four  $\Lambda_c$  and three  $\Lambda_b$  excitations. Most of their quantum numbers are undetermined, except the  $\Lambda_c(2880)$  and  $\Lambda_c(2940)$  states. The  $\Lambda_c(2880)$  was observed in 2000 by the CLEO Collaboration [96]. The Belle Collaboration later determined its quantum numbers to be  $J^P = 5/2^+$  [97]. Our calculation shows that the mass of the lowest  $5/2^+$  state is 2887/2888 MeV, which lies very close to the experimental mass. This state is dominated by the  $d_\lambda$  excited component. In 2006, the BABAR Collaboration observed the  $\Lambda_c(2940)$  in the  $D^0 p$  decay mode [98]. The LHCb Collaboration found that its quantum numbers is  $3/2^-$  [3]. From Fig. 5, we see that it is consistent with the third  $\Lambda_c$  state  $\Lambda_c(2916/2916, 3/2^-)$  with quantum numbers  $3/2^-$  within GI/MGI models. Note that Capstick and Isgur also predicted this state back in 1986. Their predicted mass was 2935 MeV [73]. The quantum numbers of  $\Lambda_c(2765)$  and  $\Lambda_c(2910)$  states are not determined. Comparing to our numerical results,  $\Lambda_c(2765)$  might be a  $1/2^+$  or  $1/2^-$  state. And the  $\Lambda_c(2910)$  is most likely a  $1/2^+$  state, though it is also possibly a  $3/2^+$  one. Now we consider the  $\Lambda_b$  baryons. Their theoretical and experimental masses are plotted together in Fig. 6. Our numerical results suggest that  $\Lambda_b(6070)$  is a  $1/2^+$  state dominated by the  $2s_\lambda$  excitation. The  $\Lambda_b(6146)$  and  $\Lambda_b(6152)$  states might belong to the  $\{3/2^+, 5/2^+\}$  or  $\{1/2^-, 3/2^-\}$  doublet. A detailed study of their decay behavior is needed.

### C. The $\Omega_Q$ baryons

Next we consider the  $\Omega_Q$  baryons. We present their masses in Table VI and plot their relative position in Figs. 9–10. The  $\Omega_Q$  system is the strange counterpart

of the  $\Sigma_Q$  system. So their mass spectra share a similar pattern.

For the  $\Omega_c$  system (see Fig. 9), the  $\Omega_c$  and  $\Omega_c^*$  are ground states, which are used for fits in this work. Next we consider the  $P$ -wave excitation with negative parity, namely the seven states lying in the 3.0 ~ 3.15 GeV mass region. Among them, the  $\Omega_c(3097/3103, 1/2^-)$  and  $\Omega_c(3132/3141, 3/2^-)$  states are dominated by the  $p_\rho$  excitations, while the others are  $p_\lambda$  one. As shown in Fig. 9, these states may correspond to the five narrow  $\Omega_c$  excited states observed by the LHCb collaboration [1]. Note that the  $\Omega_c(3020/3025, 1/2^-)$  and  $\Omega_c(3033/3041, 1/2^-)$  states are dominated by the mixing of

$$\psi_1 = |(1s_\rho, 1p_\lambda)_P, 1, 0, 1/2^- \rangle, \quad (42)$$

and

$$\psi_2 = |(1s_\rho, 1p_\lambda)_P, 1, 1, 1/2^- \rangle \quad (43)$$

bases in the notation  $|(l_\rho, l_\lambda)_L, S_{12}, j_q = L + S_{12}, J^P \rangle$ . The calculations based on  $^3P_0$  model suggested that a pure  $\psi_1$  state is very broad [ $\Gamma \sim \mathcal{O}(10^2)$  MeV] while a pure  $\psi_2$  state is very narrow ( $\Gamma \sim 0$  MeV) [99]. Since our parameters are solely fitted from the masses, we are unable to resolve the mixing angle between these two states with small mass difference. We can only say that one of the two states is broad. More precisely, the  $\Omega_c(3000)$  is a  $1/2^-$  state dominated by the  $p_\lambda$  excitation, though we cannot determine whether it corresponds to  $\Omega_c(3020/3025, 1/2^-)$  or  $\Omega_c(3033/3041, 1/2^-)$ . The  $\Omega_c(3050)$  and  $\Omega_c(3065)$  correspond to the  $\Omega_c(3054/3059, 3/2^-)$  and  $\Omega_c(3073/3080, 3/2^-)$ , which are also dominated by the  $p_\lambda$  excitations. The  $\Omega_c(3090)$  is close to  $\Omega_c(3097/3103, 1/2^-)$  and  $\Omega_c(3104/3110, 5/2^-)$  states. However, Ref. [99] suggested that the  $J^P = 1/2^-$   $p_\rho$  excitation should be a broad state ( $\sim 10^2$  MeV). Thus we interpret  $\Omega_c(3090)$  as the  $\Omega_c(3104/3110, 5/2^-)$  state, which is dominated by the  $p_\lambda$  excitation. The next state,  $\Omega_c(3120)$ , corresponds to the  $p_\rho$ -dominated excitation  $\Omega_c(3132/3143, 3/2^-)$ . In the higher mass region, the LHCb collaboration found a broad structure around 3188 MeV [1], which was later confirmed by the Belle [2] and LHCb [6] collaborations. In Ref. [6], the LHCb collaboration also found the  $\Omega_c(3327)$ . Comparing their masses with our calculated masses, we interpret the  $\Omega_c(3188)$  as the  $\Omega_c(3176/3178, 1/2^+)$  state dominated by the  $2s_\lambda$  excitation, while  $\Omega_c(3327)$  is a  $d_\lambda$ -dominated excitation with quantum numbers  $3/2^+$  or  $5/2^+$ .

Now we consider the  $\Omega_b$  system (see Fig. 10). First we consider the ground states. Only the  $1/2^+$  state is observed in experiment, while the  $3/2^-$  state,  $\Omega_b^*$ , is not observed yet. Our calculation predicts the mass of  $\Omega_b^*$  to be 6078/6077 MeV. Next we consider the  $P$ -wave excitations. Unlike the  $\Omega_c$  case, an explicit two semi-band structure appears among the  $P$ -wave  $\Omega_b$  excited states. The five lower states are dominated by  $p_\lambda$  excitations while the two higher states are dominated by  $p_\rho$  excitations. In 2020, the LHCb collaboration observed four

narrow excited  $\Omega_b$  states, namely the  $\Omega_b(6316)$ ,  $\Omega_b(6330)$ ,  $\Omega_b(6340)$ , and  $\Omega_b(6350)$  states [12]. As shown in Fig. 10, the masses of these states lie in the mass region of the  $p_\lambda$ -dominated excitations. Similar to the logic of the  $\Omega_c$  baryons, the  $\Omega_b(6316)$  is a  $1/2^-$  state. The  $\Omega_b(6330)$  and  $\Omega_b(6340)$  correspond to  $\Omega_b(6341/6347, 3/2^-)$  and  $\Omega_b(6355/6360, 3/2^-)$ . And the  $\Omega_b(6350)$  corresponds to  $\Omega_b(6369/6374, 5/2^-)$ . The  $p_\rho$ -dominated excitations is about 100 MeV above the  $p_\lambda$ -dominated excitations. In particular, the  $\Omega_b(6446/6457, 3/2^-)$ , which is the bottom counterpart of the  $\Omega_c(3120)$  state, should be a narrow state. We hope the future experiments can search for these higher states.

#### D. The $\Xi_Q$ baryons

Now we move to the  $\Xi_Q$  system with strangeness  $-1$ . Their masses are listed in Table V. The  $\Xi_Q$  baryons are composed of three different quarks, so they are not constrained by the Pauli principle. The consequence is that more bases are allowed to be mixed. In Figs. 7–8, we plot the calculated masses of the  $\Xi_Q$  baryons. We also plot the experimental states for comparison. For the  $\Xi_c$  baryons, we used the ground states and the lowest  $1/2^-$  and  $3/2^-$  states for parameter fits in Sec. III A. There are still six excited states whose quantum numbers are undetermined. From Fig. 7, we find that it is unlikely to uniquely determine their quantum numbers. The  $\Xi_c(2923)/\Xi_c(2930)$  might be a  $1/2^-$  or  $3/2^-$  state, while the  $\Xi_c(2970)$  might be a  $1/2^-$ ,  $3/2^-$  or  $5/2^-$  state. In the higher mass region, the quantum numbers of  $\Xi_c(3055)/\Xi_c(3123)$  might be  $1/2^+$  or  $3/2^+$ , while the quantum numbers of  $\Xi_c(3030)$  might be  $5/2^\pm$ . The  $\Xi_b$  baryons are similar. We used the three ground states for fits. For the higher states, the  $\Xi_b(6100)$  is most likely a  $3/2^-$  excitation, the  $\Xi_b(6227)$  could be a  $1/2^+$  or  $3/2^-$  excitation, while the quantum numbers of the  $\Xi_b(6333)$  might be  $5/2^+$ ,  $1/2^-$  or  $3/2^-$ . We hope the future experiments can determine their quantum numbers. A detailed study of their decay properties are also necessary.

#### IV. SUMMARY

In this work, we have systematically studied the masses of the heavy baryons in the relativized quark model, namely the (modified) Godfrey-Isgur [(M)GI] model. The key ingredients of the GI model are a universal one-gluon-exchange interaction and a linear confinement po-

tential motivated by QCD. The relativistic effects are included semi-quantitatively. In the MGI model, the linear confinement interaction is replaced by a screened one. The parameters are fitted from the masses of the ground state baryons, the lowest  $1/2^-$  and  $3/2^-$  singly heavy baryons and the lowest  $\frac{3}{2}^+ \Lambda_Q$  states. We found that all heavy baryons observed can be explained as three-quark states. In particular,

- (a) The  $\Omega_c(3000)$ ,  $\Omega_c(3050)$ ,  $\Omega_c(3065)$  and  $\Omega_c(3090)$  states are  $p_\lambda$ -dominated excitations with quantum numbers  $1/2^-$ ,  $3/2^-$ ,  $3/2^-$  and  $5/2^-$ , while the  $\Omega_c(3120)$  is a  $3/2^-$  state dominated the  $p_\rho$  excitation. The higher state  $\Omega_c(3188)$  is the  $2s_\lambda$  excitation with quantum numbers  $1/2^+$ , and  $\Omega_c(3327)$  is a  $d_\lambda$  excitation with quantum numbers  $3/2^+$  or  $5/2^+$ .
- (b) The  $\Omega_b(6316)$ ,  $\Omega_b(6330)$ ,  $\Omega_b(6340)$ , and  $\Omega_b(6350)$  states are  $p_\lambda$ -dominated excitations with quantum numbers  $1/2^-$ ,  $3/2^-$ ,  $3/2^-$ , and  $5/2^-$ , while a narrow  $p_\rho$ -dominated excited state  $\Omega_b(6446/6457, 3/2^-)$  is predicted to be about 100 MeV above them.
- (c) The  $\Sigma_c(2800)$  is most likely a  $3/2^-$  state dominated by the  $p_\lambda$  excitation, while the  $\Sigma_b(6097)$  is a  $1/2^-$  or  $3/2^-$  state dominated by the  $p_\lambda$  excitation.
- (d) Our calculation reproduced the masses of the well-known  $\Lambda_c(2880)$  and  $\Lambda_c(2940)$  states, whose quantum numbers are  $5/2^+$  and  $3/2^-$  respectively. The  $\Lambda_c(2765)$  might be a  $1/2^+$  or  $1/2^-$  state, and the  $\Lambda_c(2910)$  could be a  $1/2^+$  or  $3/2^+$  one. Furthermore, the  $\Lambda_b(6070)$  is a  $1/2^+$  state dominated by the  $2s_\lambda$  excitation, while the  $\Lambda_b(6146)$  and  $\Lambda_b(6152)$  states might belong to the  $\{3/2^+, 5/2^+\}$  or  $\{1/2^-, 3/2^-\}$  doublet.

Hopefully, our calculations will be useful for the search of the new baryon states. More experimental and theoretical investigations are expected to verify and understand the baryon system in the future.

#### ACKNOWLEDGMENTS

We are grateful to Prof. Marek Karliner, Prof. Guang-Juan Wang and Dr. Lu Meng for helpful comments and discussions. We thank the High-performance Computing Platform of Peking University for providing computational resources. This project was supported by the National Natural Science Foundation of China (NSFC) under Grant No. 11975033 and No. 12070131001; and the NSFC-ISF under Grant No. 3423/19.

[1] R. Aaij *et al.* (LHCb Collaboration), Observation of Five New Narrow  $\Omega_c^0$  States Decaying to  $\Xi_c^+ K^-$ , *Phys. Rev. Lett.* **118**, 182001 (2017), arXiv:1703.04639 [hep-ex].

[2] J. Yelton *et al.* (Belle Collaboration), Observation of excited  $\Omega_c$  charmed baryons in  $e^+e^-$  collisions, *Phys. Rev. D* **97**, 051102 (2018), arXiv:1711.07927 [hep-ex].



TABLE III. Masses of  $\Lambda_c$  and  $\Sigma_c$  baryons (in units of MeV).

State	$J^P$	Model	Mass
$\Lambda_c$	$1/2^+$	GI	2290 2772 2921 3007 3041 3101 3155 3185 3326 3389
		MGI	2288 2772 2902 3014 3041 3135 3164 3173 3306 3379
	$3/2^+$	GI	2870 2941 3054 3094 3169 3196 3218 3238 3338
		MGI	2871 2926 3066 3117 3177 3197 3208 3237 3319
	$5/2^+$	GI	2887 3120 3186 3228 3246 3263
		MGI	2888 3140 3184 3217 3239 3273
	$7/2^+$	GI	3219 3322
		MGI	3214 3308
	$9/2^+$	GI	3324
		MGI	3311
	$1/2^-$	GI	2594 2622 2767 3022 3115 3205 3260 3298 3323 3350 3359 3390
		MGI	2592 2599 2782 3016 3098 3208 3254 3292 3324 3337 3355 3383
	$3/2^-$	GI	2624 2826 2916 3036 3202 3235 3267 3287 3336 3349 3368
		MGI	2627 2849 2916 3028 3192 3236 3266 3281 3335 3343 3367
	$5/2^-$	GI	2973 3119 3216 3313 3350 3367
		MGI	2973 3114 3209 3312 3361 3364
	$7/2^-$	GI	3126 3355
		MGI	3122 3358
$\Sigma_c$	$1/2^+$	GI	2439 2925 3025 3035 3096 3119 3165 3323 3377 3404 3457 3488
		MGI	2437 2923 3032 3040 3112 3118 3180 3305 3364 3383 3431 3480
	$3/2^+$	GI	2519 2973 3030 3044 3124 3139 3151 3176 3193 3348 3376 3389 3473 3480 3492
		MGI	2518 2969 3027 3054 3135 3143 3168 3189 3217 3328 3354 3377 3453 3457 3477
	$5/2^+$	GI	3040 3091 3165 3227 3233 3384 3418 3478 3485
		MGI	3036 3092 3181 3220 3248 3360 3394 3458 3476
	$7/2^+$	GI	3109 3280 3431 3460 3485
		MGI	3109 3269 3406 3440 3479
	$9/2^+$	GI	3459
		MGI	3440
	$1/2^-$	GI	2751 2764 2845 3158 3166 3246 3290 3304 3329 3394 3401 3423 3451
		MGI	2753 2773 2852 3149 3162 3244 3287 3305 3338 3387 3410 3433 3480
	$3/2^-$	GI	2787 2820 2890 3177 3197 3268 3273 3308 3325 3366 3370 3408 3420 3442 3447 3459 3486
		MGI	2788 2825 2905 3167 3189 3263 3276 3300 3314 3371 3380 3404 3422 3452 3455 3485 3489
	$5/2^-$	GI	2857 3223 3258 3278 3348 3372 3391 3431 3440 3456 3496
		MGI	2861 3212 3248 3284 3334 3382 3395 3437 3445 3466 3487
	$7/2^-$	GI	3261 3317 3392 3450 3463
		MGI	3251 3309 3395 3436 3472
$9/2^-$	GI	3324 3483	
	MGI	3315 3464	

TABLE IV. Masses of  $\Lambda_b$  and  $\Sigma_b$  baryons (in units of MeV).

State	$J^P$	Model	Mass
$\Lambda_b$	$1/2^+$	GI	5625 6047 6214 6325 6357 6406 6429 6472 6572 6659 6661
		MGI	5623 6047 6195 6339 6353 6406 6457 6483 6555 6636 6660
	$3/2^+$	GI	6130 6225 6342 6390 6450 6478 6528 6552 6579 6670 6693
		MGI	6130 6207 6357 6412 6442 6488 6524 6562 6568 6670 6672
	$5/2^+$	GI	6140 6403 6456 6493 6537 6570 6650
		MGI	6141 6425 6448 6490 6534 6586 6639 6676
	$7/2^+$	GI	6505 6525 6657
		MGI	6503 6518 6647
	$9/2^+$	GI	6530
		MGI	6523
	$1/2^-$	GI	5894 5952 6122 6271 6389 6502 6541 6578 6616 6624 6653 6679 6696
		MGI	5896 5922 6141 6268 6373 6509 6528 6571 6618 6639 6648 6674 6685
	$3/2^-$	GI	5906 6146 6274 6282 6460 6514 6545 6559 6581 6635 6641 6685
		MGI	5908 6167 6273 6279 6450 6521 6532 6570 6575 6639 6653 6689
	$5/2^-$	GI	6294 6348 6468 6570 6602 6616 6653
		MGI	6295 6347 6460 6582 6588 6629 6650
$7/2^-$	GI	6355 6609 6620 6685	
	MGI	6354 6594 6633 6677	
$9/2^-$	GI	6681 6697	
	MGI	6666 6687	
$\Sigma_b$	$1/2^+$	GI	5809 6237 6313 6332 6439 6446 6479 6578 6620 6661 6743 6762 6802 6837 6844 6846 6873 6880 6883
		MGI	5809 6236 6324 6337 6442 6459 6502 6565 6616 6653 6726 6760 6803 6822 6834 6847 6854 6876 6883 6898
	$3/2^+$	GI	5838 6253 6307 6322 6437 6454 6458 6491 6527 6585 6610 6627 6724 6753 6765 6777 6810 6829 6847 6856
		MGI	5838 6252 6306 6334 6451 6454 6473 6519 6545 6572 6596 6622 6719 6736 6763 6771 6811 6827 6841 6852
	$5/2^+$	GI	6314 6352 6448 6547 6582 6615 6642 6704 6730 6783 6813 6839 6840 6877 6891 6897
		MGI	6313 6354 6465 6567 6573 6601 6629 6707 6723 6778 6795 6836 6845 6858 6869 6879 6887
	$7/2^+$	GI	6362 6600 6650 6680 6709 6822 6825 6843 6897
		MGI	6364 6590 6637 6669 6713 6804 6826 6849 6883 6895
	$9/2^+$	GI	6684 6725 6828
		MGI	6674 6716 6829
	$1/2^-$	GI	6075 6081 6195 6430 6438 6535 6587 6595 6631 6696 6700 6729 6742 6750 6763 6830 6890 6898
		MGI	6080 6090 6207 6424 6440 6537 6591 6597 6645 6697 6706 6723 6738 6739 6793 6818 6874 6880
	$3/2^-$	GI	6090 6119 6212 6436 6453 6520 6544 6603 6627 6647 6659 6701 6707 6736 6746 6748 6761 6768 6788 6802
		MGI	6092 6122 6227 6431 6448 6529 6545 6601 6618 6660 6668 6703 6718 6728 6740 6748 6753 6790 6797 6806
	$5/2^-$	GI	6134 6464 6503 6527 6639 6645 6664 6711 6733 6754 6768 6784 6796 6808 6818 6846
		MGI	6138 6458 6498 6536 6629 6657 6673 6728 6748 6749 6759 6763 6797 6805 6814 6850 6884 6899
	$7/2^-$	GI	6508 6548 6651 6745 6760 6789 6825 6827 6863 6879
		MGI	6504 6545 6663 6745 6760 6767 6798 6814 6868 6871 6887
	$9/2^-$	GI	6554 6772 6830 6851 6883
		MGI	6552 6757 6803 6830 6875





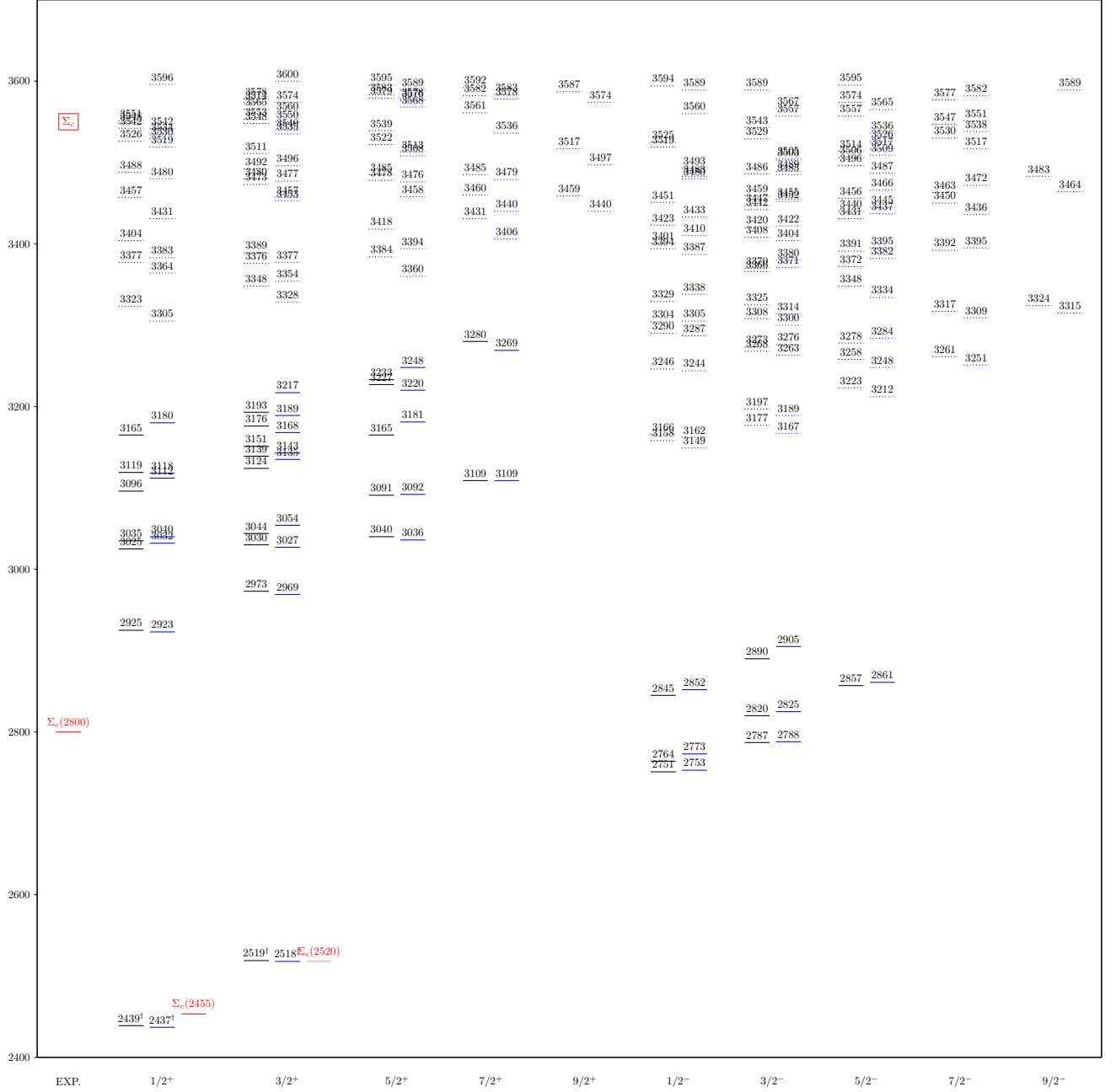


FIG. 3. Masses of the  $\Sigma_c$  baryons (in units of MeV). Here, the black/blue lines stand for the numerical results obtained by the GI/MGI models. The red lines represent the experimental results taken from PDG [15]. In the first column, we list the experimental observed states whose quantum numbers are not determined yet. The states used for fittings are indicated by daggers ( $\dagger$ ).

- [3] R. Aaij *et al.* (LHCb Collaboration), Study of the  $D^0 p$  amplitude in  $\Lambda_b^0 \rightarrow D^0 p \pi^-$  decays, *JHEP* **05**, 030, arXiv:1701.07873 [hep-ex].
- [4] R. Aaij *et al.* (LHCb Collaboration), Observation of New  $\Xi_c^0$  Baryons Decaying to  $\Lambda_c^+ K^-$ , *Phys. Rev. Lett.* **124**, 222001 (2020), arXiv:2003.13649 [hep-ex].
- [5] Y. B. Li *et al.* (Belle Collaboration), Evidence of a New Excited Charmed Baryon Decaying to  $\Sigma_c(2455)^{0,++} \pi^\pm$ , *Phys. Rev. Lett.* **130**, 031901 (2023), arXiv:2206.08822 [hep-ex].
- [6] R. Aaij *et al.* (LHCb Collaboration), Observation of New  $\Omega_c^0$  States Decaying to the  $\Xi_c^+ K^-$  Final State, *Phys. Rev. Lett.* **131**, 131902 (2023), arXiv:2302.04733 [hep-ex].
- [7] R. Aaij *et al.* (LHCb Collaboration), Observation of Two Resonances in the  $\Lambda_b^0 \pi^\pm$  Systems and Precise Measurement of  $\Sigma_b^\pm$  and  $\Sigma_b^{*\pm}$  Properties, *Phys. Rev. Lett.* **122**, 012001 (2019), arXiv:1809.07752 [hep-ex].

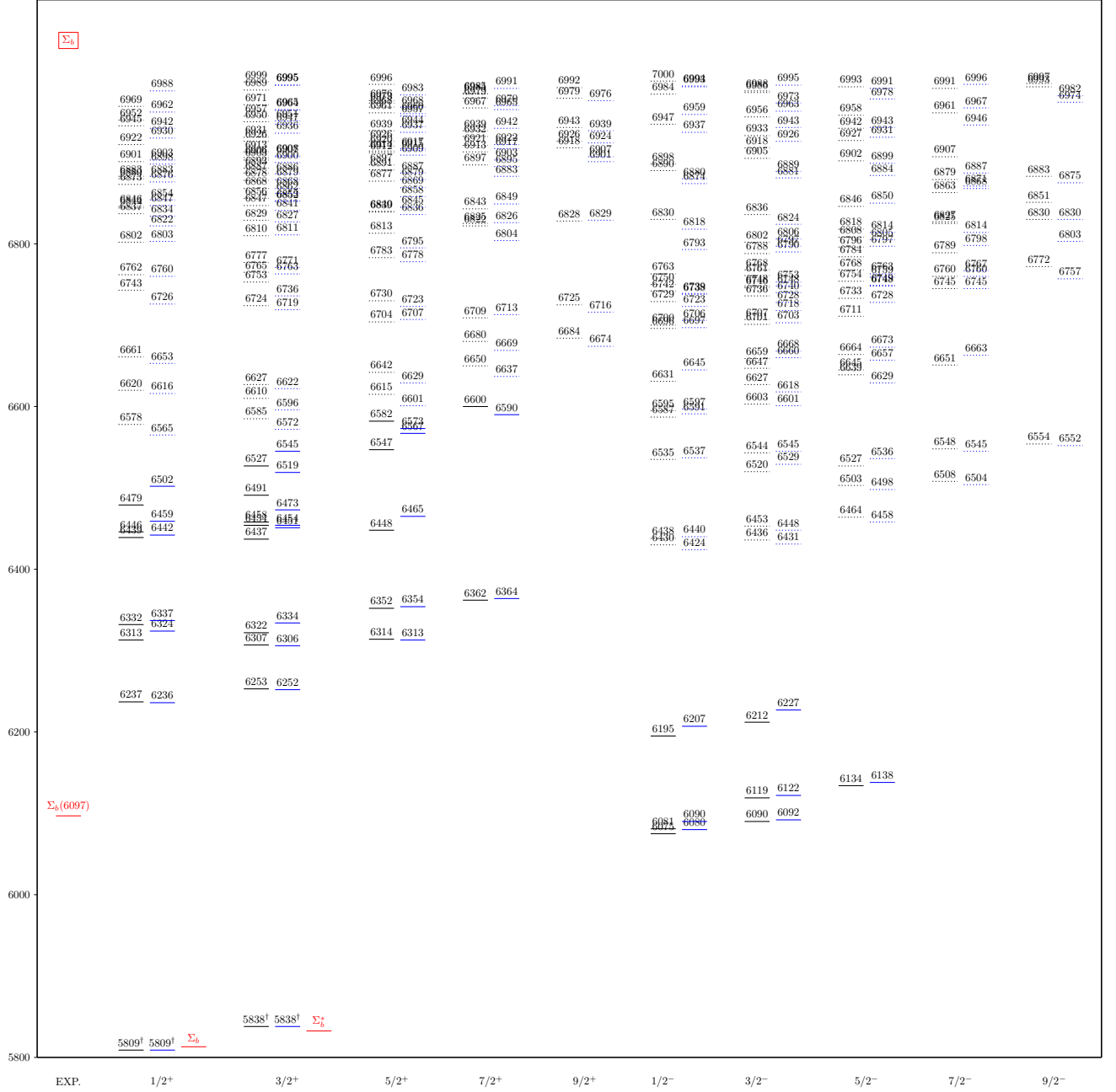


FIG. 4. Masses of the  $\Sigma_b$  baryons (in units of MeV). Here, the black/blue lines stand for the numerical results obtained by the GI/MGI models. The red lines represent the experimental results taken from PDG [15]. In the first column, we list the experimental observed states whose quantum numbers are not determined yet. The states used for fittings are indicated by daggers (†).

- [8] R. Aaij *et al.* (LHCb Collaboration), Observation of a New  $\Xi_b^-$  Resonance, *Phys. Rev. Lett.* **121**, 072002 (2018), arXiv:1805.09418 [hep-ex].
- [9] R. Aaij *et al.* (LHCb Collaboration), Observation of a new  $\Xi_b^0$  state, *Phys. Rev. D* **103**, 012004 (2021), arXiv:2010.14485 [hep-ex].
- [10] R. Aaij *et al.* (LHCb Collaboration), Observation of New Resonances in the  $\Lambda_b^0 \pi^+ \pi^-$  System, *Phys. Rev. Lett.* **123**, 152001 (2019), arXiv:1907.13598 [hep-ex].
- [11] A. M. Sirunyan *et al.* (CMS Collaboration), Study of excited  $\Lambda_b^0$  states decaying to  $\Lambda_b^0 \pi^+ \pi^-$  in proton-proton collisions at  $\sqrt{s} = 13$  TeV, *Phys. Lett. B* **803**, 135345 (2020), arXiv:2001.06533 [hep-ex].
- [12] R. Aaij *et al.* (LHCb Collaboration), First Observation of Excited  $\Omega_b^-$  States, *Phys. Rev. Lett.* **124**, 082002 (2020), arXiv:2001.00851 [hep-ex].
- [13] A. M. Sirunyan *et al.* (CMS Collaboration), Observation of a New Excited Beauty Strange Baryon Decay-

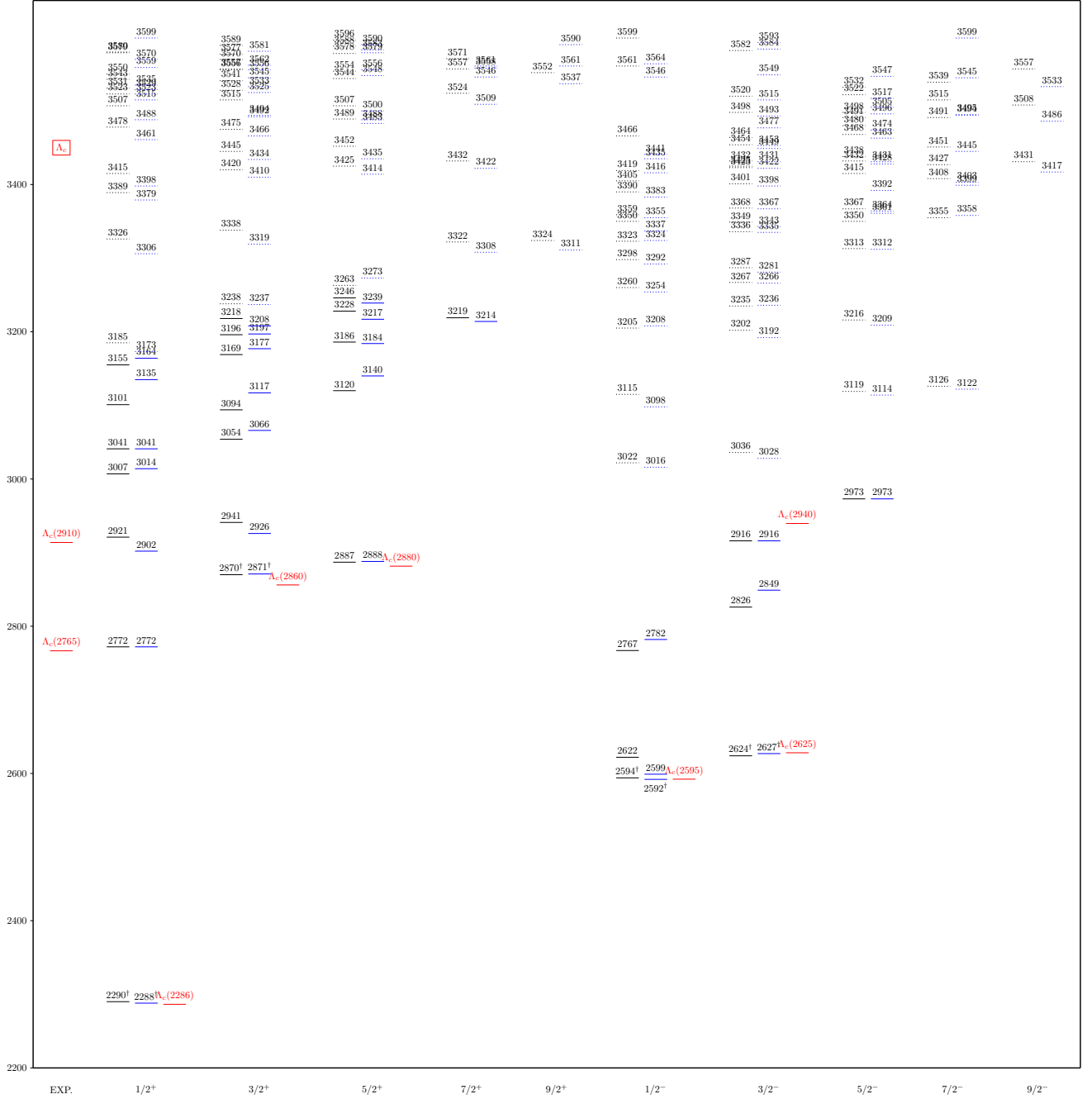


FIG. 5. Masses of the  $\Lambda_c$  baryons (in units of MeV). Here, the black/blue lines stand for the numerical results obtained by the GI/MGI models. The red lines represent the experimental results taken from PDG [15] and Ref. [5]. In the first column, we list the experimental observed states whose quantum numbers are not determined yet. The states used for fittings are indicated by daggers ( $\dagger$ ).

- ing to  $\Xi_b^- \pi^+ \pi^-$ , *Phys. Rev. Lett.* **126**, 252003 (2021), [arXiv:2102.04524 \[hep-ex\]](https://arxiv.org/abs/2102.04524).
- [14] R. Aaij *et al.* (LHCb Collaboration), Observation of Two New Excited  $\Xi_b^0$  States Decaying to  $\Lambda_b^0 K^- \pi^+$ , *Phys. Rev. Lett.* **128**, 162001 (2022), [arXiv:2110.04497 \[hep-ex\]](https://arxiv.org/abs/2110.04497).
- [15] R. L. Workman *et al.* (Particle Data Group), Review of Particle Physics, *PTEP* **2022**, 083C01 (2022).
- [16] N. Isgur and G. Karl, Hyperfine interactions in negative parity baryons, *Phys. Lett.* **72B**, 109 (1977).
- [17] N. Isgur and G. Karl, Positive-parity excited baryons in a quark model with hyperfine interactions, *Phys. Rev.* **D19**, 2653 (1979), [Erratum: *Phys. Rev.* **D23**, 817 (1981)].
- [18] A. Martin and J.-M. Richard,  $\Omega_c$  and other charmed baryons revisited, *Phys. Lett.* **B355**, 345 (1995), [arXiv:hep-ph/9504276 \[hep-ph\]](https://arxiv.org/abs/hep-ph/9504276).

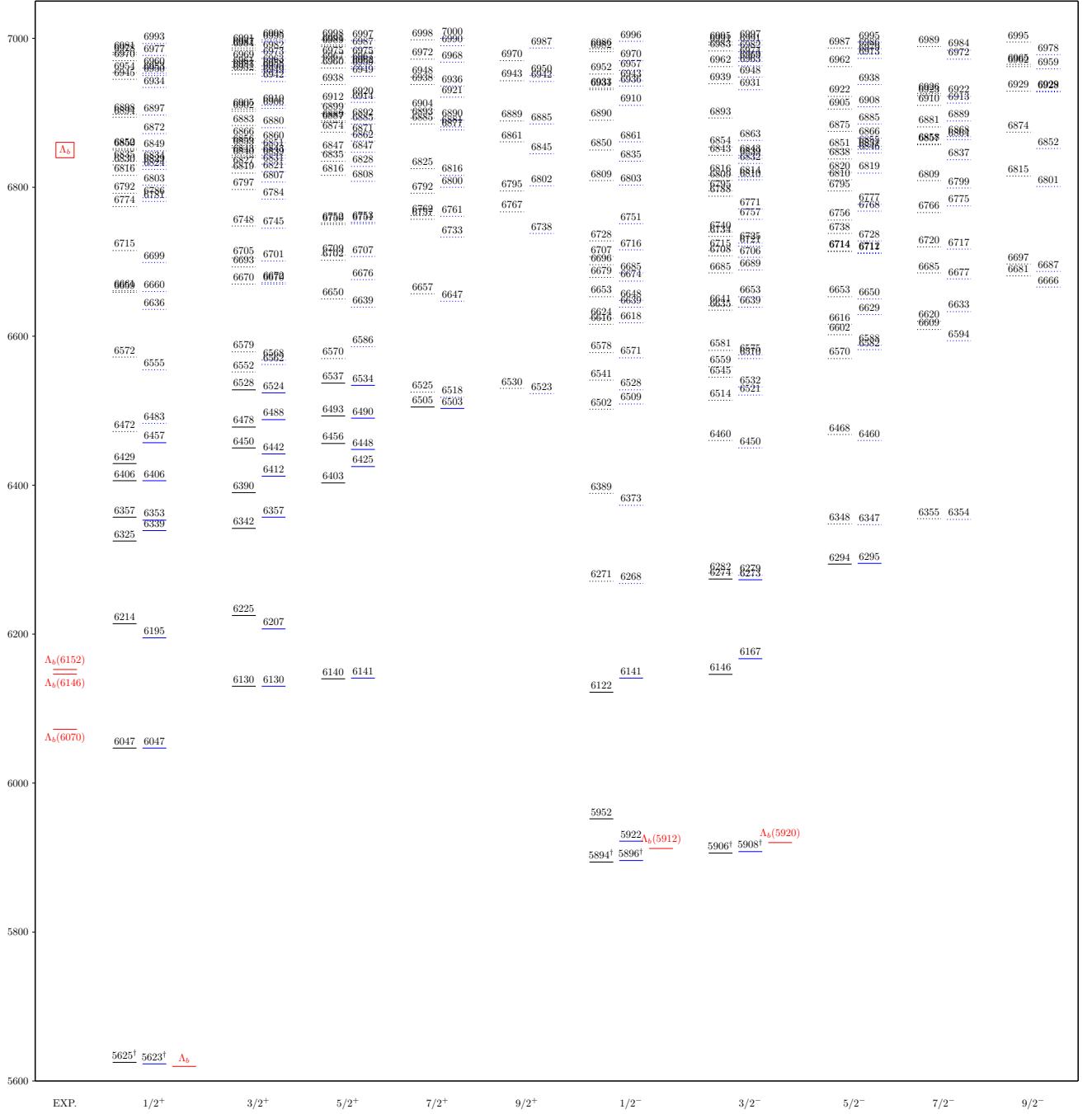


FIG. 6. Masses of the  $\Lambda_b$  baryons (in units of MeV). Here, the black/blue lines stand for the numerical results obtained by the GI/MGI models. The red lines represent the experimental results taken from PDG [15]. In the first column, we list the experimental observed states whose quantum numbers are not determined yet. The states used for fittings are indicated by daggers ( $\dagger$ ).

- [19] D. Ebert, R. N. Faustov, and V. O. Galkin, Masses of heavy baryons in the relativistic quark model, *Phys. Rev. D* **72**, 034026 (2005), arXiv:hep-ph/0504112 [hep-ph].
- [20] D. Ebert, R. N. Faustov, and V. O. Galkin, Masses of excited heavy baryons in the relativistic quark-diquark picture, *Phys. Lett. B* **659**, 612 (2008), arXiv:0705.2957 [hep-ph].

- [21] W. Roberts and M. Pervin, Heavy baryons in a quark model, *Int. J. Mod. Phys. A* **23**, 2817 (2008), arXiv:0711.2492 [nucl-th].
- [22] M. Karliner, B. Keren-Zur, H. J. Lipkin, and J. L. Rosner, The quark model and  $b$  baryons, *Annals Phys.* **324**, 2 (2009), arXiv:0804.1575 [hep-ph].



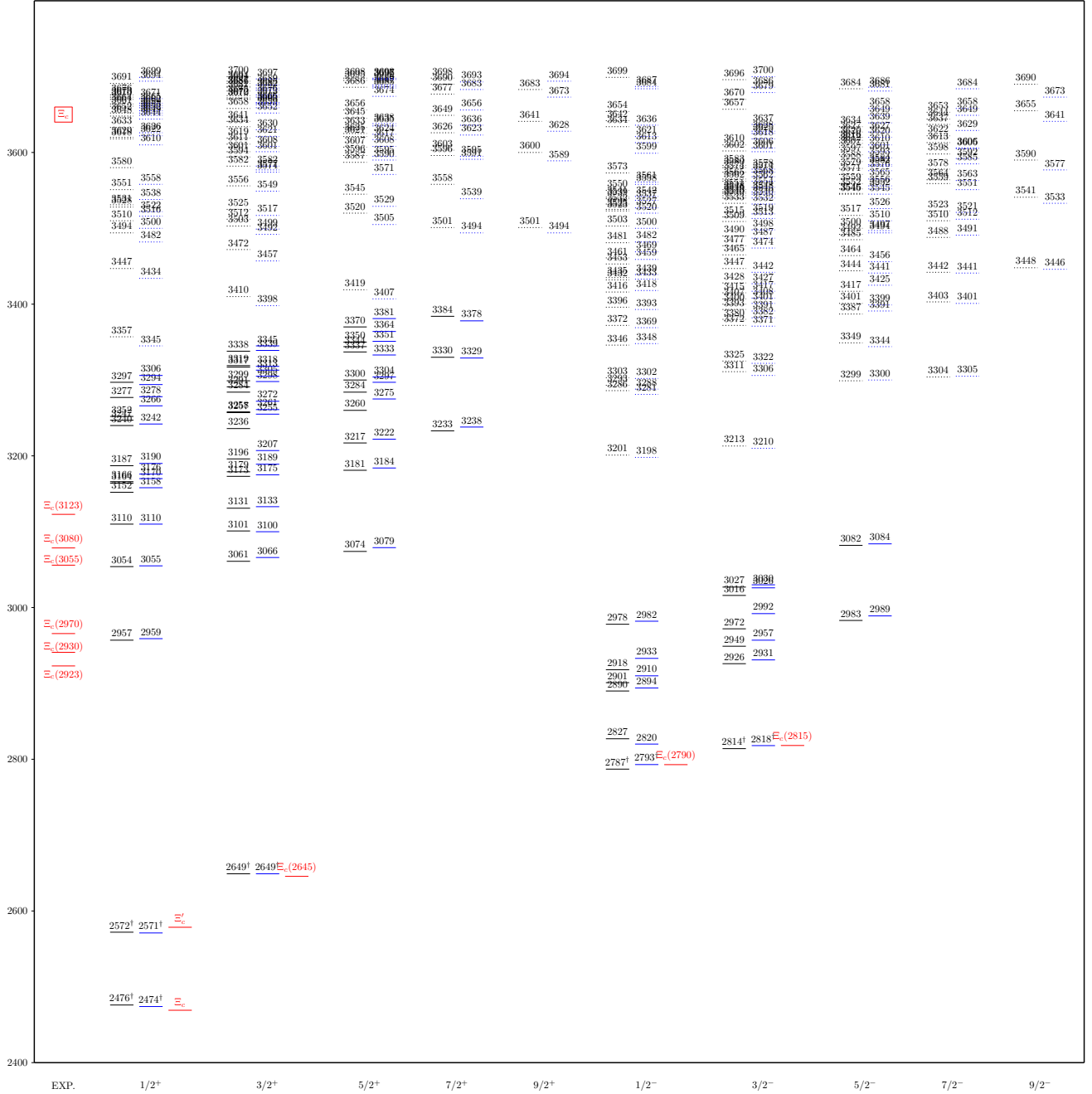


FIG. 7. Masses of the  $\Xi_c$  baryons (in units of MeV). Here, the black/blue lines stand for the numerical results obtained by the GI/MGI models. The red lines represent the experimental results taken from PDG [15]. In the first column, we list the experimental observed states whose quantum numbers are not determined yet. The states used for fittings are indicated by daggers ( $\dagger$ ).

- [23] A. Valcarce, H. Garcilazo, and J. Vijande, Towards an understanding of heavy baryon spectroscopy, *Eur. Phys. J. A* **37**, 217 (2008), arXiv:0807.2973 [hep-ph].
- [24] Y. Yang, C. Deng, H. Huang, and J. Ping, Dynamical study of heavy-baryon spectroscopy, *Mod. Phys. Lett. A* **23**, 1819 (2008).
- [25] J. Vijande, A. Valcarce, and H. Garcilazo, Heavy-baryon quark model picture from lattice QCD, *Phys. Rev. D* **90**, 094004 (2014), arXiv:1507.03736 [hep-ph].
- [26] M. Karliner and J. L. Rosner, Prospects for observing the lowest-lying odd-parity  $\Sigma_c$  and  $\Sigma_b$  baryons, *Phys. Rev. D* **92**, 074026 (2015), arXiv:1506.01702 [hep-ph].
- [27] M. Karliner and J. L. Rosner, Very narrow excited  $\omega_c$  baryons, *Phys. Rev. D* **95**, 114012 (2017), arXiv:1703.07774 [hep-ph].

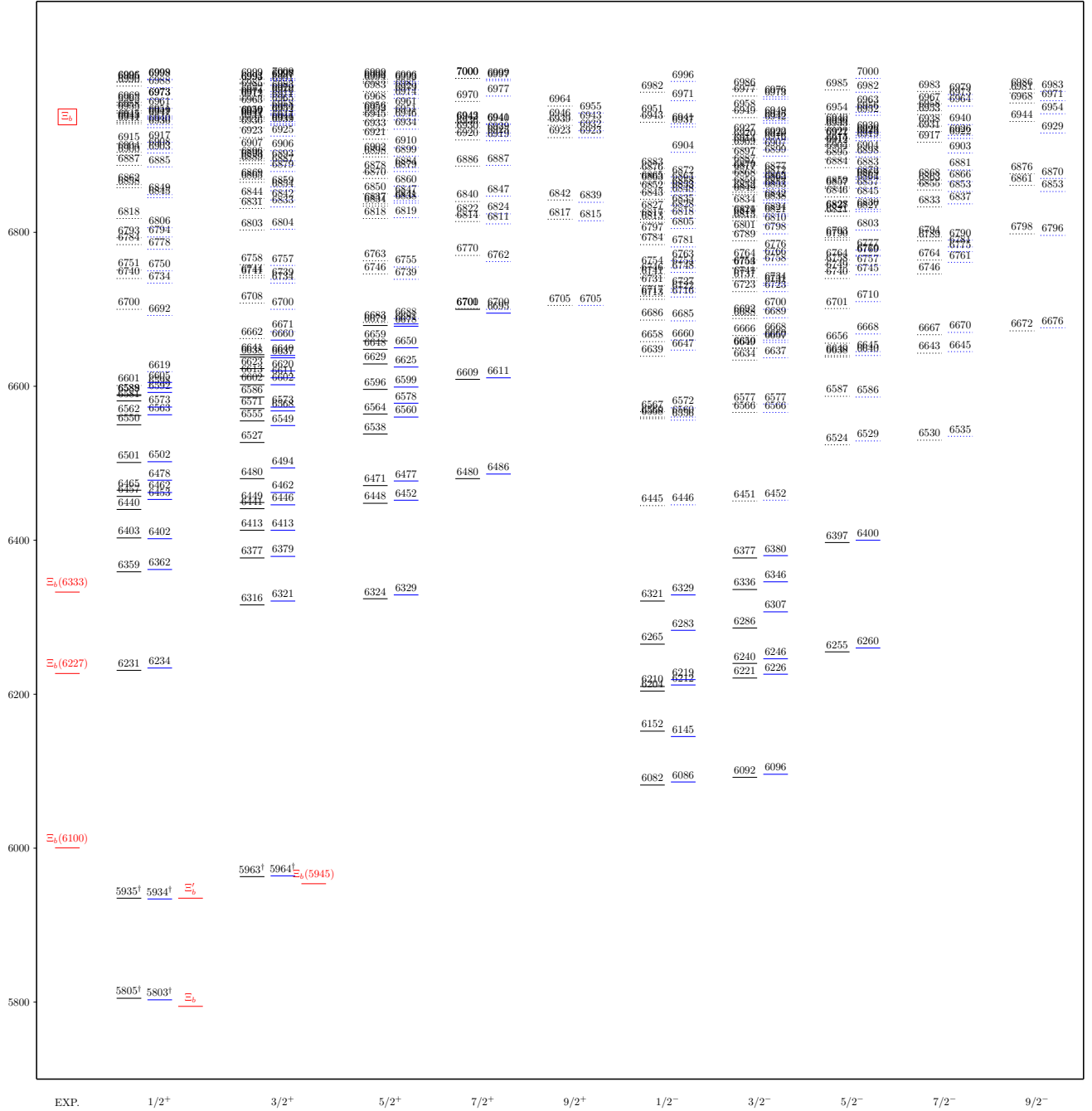


FIG. 8. Masses of the  $\Xi_b$  baryons (in units of MeV). Here, the black/blue lines stand for the numerical results obtained by the GI/MGI models. The red lines represent the experimental results taken from PDG [15]. In the first column, we list the experimental observed states whose quantum numbers are not determined yet. The states used for fittings are indicated by daggers ( $\dagger$ ).

- [28] K.-L. Wang, Y.-X. Yao, X.-H. Zhong, and Q. Zhao, Strong and radiative decays of the low-lying  $S$ - and  $P$ -wave singly heavy baryons, *Phys. Rev.* **D96**, 116016 (2017), arXiv:1709.04268 [hep-ph].
- [29] G. Yang, J. Ping, and J. Segovia, The  $S$ - and  $P$ -Wave Low-Lying Baryons in the Chiral Quark Model, *Few Body Syst.* **59**, 113 (2018), arXiv:1709.09315 [hep-ph].

- [30] M. Karliner and J. L. Rosner, Scaling of  $P$ -wave excitation energies in heavy-quark systems, *Phys. Rev.* **D98**, 074026 (2018), arXiv:1808.07869 [hep-ph].
- [31] S. Shi, J. Zhao, and P. Zhuang, Heavy flavor dissociation in framework of multi-body Dirac equations, *Chin. Phys.* **C44**, 8 (2020), arXiv:1905.10627 [nucl-th].

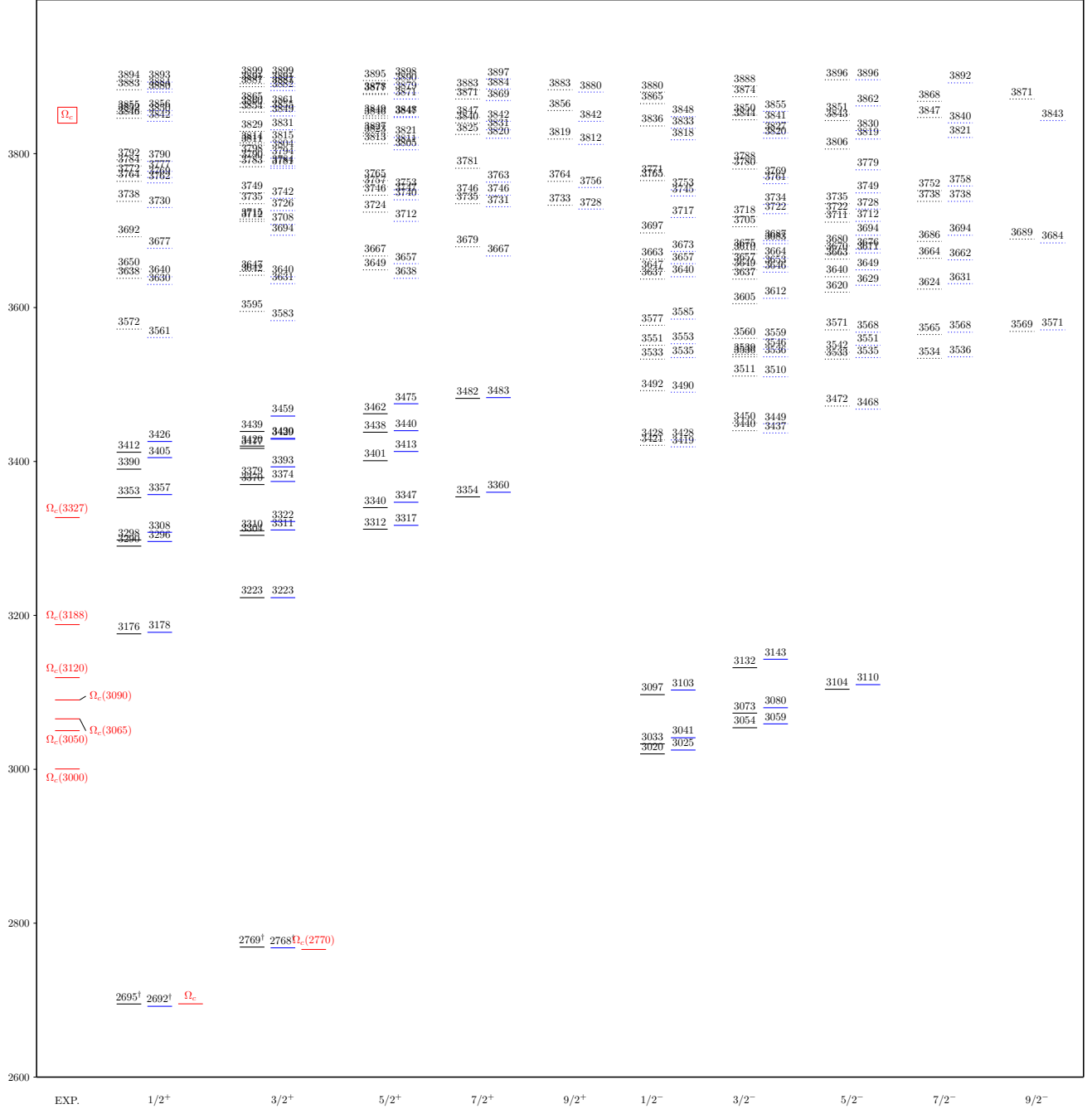


FIG. 9. Masses of the  $\Omega_c$  baryons (in units of MeV). Here, the black/blue lines stand for the numerical results obtained by the GI/MGI models. The red lines represent the experimental results taken from PDG [15]. In the first column, we list the experimental observed states whose quantum numbers are not determined yet. The states used for fittings are indicated by daggers ( $\dagger$ ).

[32] M. Karliner and J. L. Rosner, Interpretation of excited  $\Omega_b$  signals, *Phys. Rev.* **D102**, 014027 (2020), arXiv:2005.12424 [hep-ph].

[33] K.-L. Wang, L.-Y. Xiao, and X.-H. Zhong, Understanding the newly observed  $\Xi_c^0$  states through their decays, *Phys. Rev.* **D102**, 034029 (2020), arXiv:2004.03221 [hep-ph].

[34] L.-Y. Xiao and X.-H. Zhong, Toward establishing the low-lying  $P$ -wave  $\Sigma_b$  states, *Phys. Rev.* **D102**, 014009 (2020), arXiv:2004.11106 [hep-ph].

[35] B. Chen, S.-Q. Luo, and X. Liu, Universal behavior of mass gaps existing in the single heavy baryon family, *Eur. Phys. J. C* **81**, 474 (2021), arXiv:2101.10806 [hep-ph].

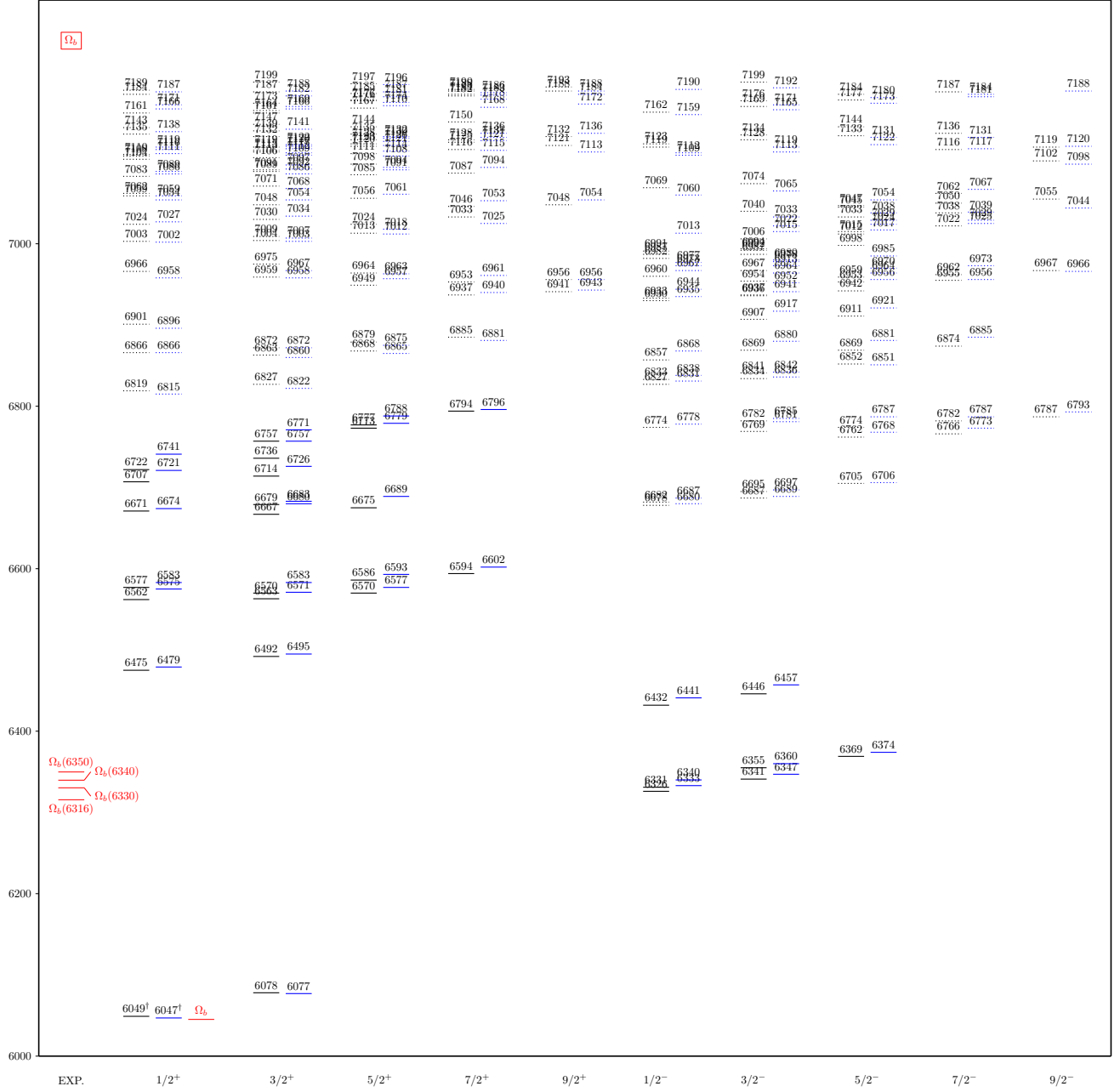


FIG. 10. Masses of the  $\Omega_b$  baryons (in units of MeV). Here, the black/blue lines stand for the numerical results obtained by the GI/MGI models. The red lines represent the experimental results taken from PDG [15]. In the first column, we list the experimental observed states whose quantum numbers are not determined yet. The states used for fittings are indicated by daggers ( $\dagger$ ).

- [36] K.-L. Wang and X.-H. Zhong, Toward discovering low-lying  $P$ -wave excited  $\Sigma_c$  baryon states, *Chin. Phys. C* **46**, 023103 (2022), arXiv:2110.12443 [hep-ph].
- [37] H. García-Tecocoatzi, A. Giachino, J. Li, A. Ramirez-Morales, and E. Santopinto, Strong decay widths and mass spectra of charmed baryons, *Phys. Rev. D* **107**, 034031 (2023), arXiv:2205.07049 [hep-ph].
- [38] Y. Ma, L. Meng, Y.-K. Chen, and S.-L. Zhu, Ground state baryons in the flux-tube three-body confinement model using diffusion Monte Carlo, *Phys. Rev. D* **107**, 054035 (2023), arXiv:2211.09021 [hep-ph].
- [39] W.-J. Wang, L.-Y. Xiao, and X.-H. Zhong, Strong decays of the low-lying  $\rho$ -mode  $1P$ -wave singly heavy baryons, *Phys. Rev. D* **106**, 074020 (2022), arXiv:2208.10116 [hep-ph].
- [40] M. Karliner and J. L. Rosner, Excited  $\Omega_c$  Baryons as  $2S$  states, *Phys. Rev. D* **108**, 014006 (2023), arXiv:2304.00407 [hep-ph].

- [41] E. Ortiz-Pacheco and R. Bijker, Heavy  $\Xi_{c/b}$  and  $\Xi'_{c/b}$  baryons in the quark model, *J. Phys. Conf. Ser.* **2619**, 012011 (2023), arXiv:2309.12266 [hep-ph].
- [42] L. Liu, H.-W. Lin, K. Orginos, and A. Walker-Loud, Singly and Doubly Charmed  $J=1/2$  Baryon Spectrum from Lattice QCD, *Phys. Rev. D* **81**, 094505 (2010), arXiv:0909.3294 [hep-lat].
- [43] R. A. Briceño, H.-W. Lin, and D. R. Bolton, Charmed-baryon spectroscopy from lattice QCD with  $N_f=2+1+1$  flavors, *Phys. Rev. D* **86**, 094504 (2012), arXiv:1207.3536 [hep-lat].
- [44] Y. Namekawa, S. Aoki, K.-I. Ishikawa, N. Ishizuka, K. Kanaya, Y. Kuramashi, M. Okawa, Y. Taniguchi, A. Ukawa, N. Ukita, and T. Yoshié (PACS-CS Collaboration), Charmed baryons at the physical point in 2+1 flavor lattice QCD, *Phys. Rev. D* **87**, 094512 (2013), arXiv:1301.4743 [hep-lat].
- [45] Z. S. Brown, W. Detmold, S. Meinel, and K. Orginos, Charmed bottom baryon spectroscopy from lattice QCD, *Phys. Rev. D* **90**, 094507 (2014), arXiv:1409.0497 [hep-lat].
- [46] P. Pérez-Rubio, S. Collins, and G. S. Bali, Charmed baryon spectroscopy and light flavor symmetry from lattice QCD, *Phys. Rev. D* **92**, 034504 (2015), arXiv:1503.08440 [hep-lat].
- [47] H. Bahtiyar, K. U. Can, G. Erkol, P. Gubler, M. Oka, and T. T. Takahashi (TRJQCD Collaboration), Charmed baryon spectrum from lattice QCD near the physical point, *Phys. Rev. D* **102**, 054513 (2020), arXiv:2004.08999 [hep-lat].
- [48] Q.-A. Zhang, J. Hua, F. Huang, R. Li, Y. Li, C.-D. Lu, P. Sun, W. Sun, W. Wang, and Y.-B. Yang, First lattice QCD calculation of semileptonic decays of charmed-strange baryons  $\Xi_c$ , *Chin. Phys. C* **46**, 011002 (2022), arXiv:2103.07064 [hep-lat].
- [49] E. Bagan, M. Chabab, H. G. Dosch, and S. Narison, Spectra of heavy baryons from QCD spectral sum rules, *Phys. Lett. B* **287**, 176 (1992).
- [50] Z.-G. Wang, Reanalysis of the heavy baryon states  $\Omega(b)$ ,  $\Omega(c)$ ,  $\Xi'(b)$ ,  $\Xi'(c)$ ,  $\Sigma(b)$  and  $\Sigma(c)$  with QCD sum rules, *Phys. Lett. B* **685**, 59 (2010), arXiv:0912.1648 [hep-ph].
- [51] J.-R. Zhang and M.-Q. Huang, Heavy flavor baryon spectra via QCD sum rules, *Chin. Phys. C* **33**, 1385 (2009), arXiv:0904.3391 [hep-ph].
- [52] H.-X. Chen, W. Chen, Q. Mao, A. Hosaka, X. Liu, and S.-L. Zhu,  $P$ -wave charmed baryons from QCD sum rules, *Phys. Rev. D* **91**, 054034 (2015), arXiv:1502.01103 [hep-ph].
- [53] Q. Mao, H.-X. Chen, W. Chen, A. Hosaka, X. Liu, and S.-L. Zhu, QCD sum rule calculation for  $P$ -wave bottom baryons, *Phys. Rev. D* **92**, 114007 (2015), arXiv:1510.05267 [hep-ph].
- [54] S. S. Agaev, K. Azizi, and H. Sundu, Interpretation of the new  $\omega_c^0$  states via their mass and width, *Eur. Phys. J. C* **77**, 395 (2017), arXiv:1704.04928 [hep-ph].
- [55] H.-M. Yang, H.-X. Chen, E.-L. Cui, and Q. Mao, Identifying the  $\Xi_b(6100)$  as the  $P$ -wave bottom baryon of  $J^P = 3/2^-$ , *Phys. Rev. D* **106**, 036018 (2022), arXiv:2205.07224 [hep-ph].
- [56] K. K. Vishwakarma and A. Upadhyay, Masses of 2S single heavy baryons using non-perturbative parameters in HQET, (2022), arXiv:2208.02536 [hep-ph].
- [57] K.-W. Wei, B. Chen, N. Liu, Q.-Q. Wang, and X.-H. Guo, Spectroscopy of singly, doubly, and triply bottom baryons, *Phys. Rev. D* **95**, 116005 (2017), arXiv:1609.02512 [hep-ph].
- [58] D. Jia, W.-N. Liu, and A. Hosaka, Regge behaviors in orbitally excited spectroscopy of charmed and bottom baryons, *Phys. Rev. D* **101**, 034016 (2020), arXiv:1907.04958 [hep-ph].
- [59] J. Oudichhya and A. K. Rai, Spin-parity identification of newly observed singly charmed baryons in Regge phenomenology, *Eur. Phys. J. A* **59**, 123 (2023).
- [60] E. Klempt and J.-M. Richard, Baryon spectroscopy, *Rev. Mod. Phys.* **82**, 1095 (2010), arXiv:0901.2055 [hep-ph].
- [61] V. Crede and W. Roberts, Progress towards understanding baryon resonances, *Rept. Prog. Phys.* **76**, 076301 (2013), arXiv:1302.7299 [nucl-ex].
- [62] H.-X. Chen, W. Chen, X. Liu, Y.-R. Liu, and S.-L. Zhu, A review of the open charm and open bottom systems, *Rept. Prog. Phys.* **80**, 076201 (2017), arXiv:1609.08928 [hep-ph].
- [63] G. Eichmann, H. Sanchis-Alepuz, R. Williams, R. Alkofer, and C. S. Fischer, Baryons as relativistic three-quark bound states, *Prog. Part. Nucl. Phys.* **91**, 1 (2016), arXiv:1606.09602 [hep-ph].
- [64] H.-Y. Cheng, Charmed baryon physics circa 2021, *Chin. J. Phys.* **78**, 324 (2022), arXiv:2109.01216 [hep-ph].
- [65] H.-X. Chen, W. Chen, X. Liu, Y.-R. Liu, and S.-L. Zhu, An updated review of the new hadron states, *Rept. Prog. Phys.* **86**, 026201 (2023), arXiv:2204.02649 [hep-ph].
- [66] S. Godfrey and N. Isgur, Mesons in a relativized quark model with chromodynamics, *Phys. Rev. D* **32**, 189 (1985).
- [67] S. Godfrey and R. Kokoski, Properties of  $P$ -wave mesons with one heavy quark, *Phys. Rev. D* **43**, 1679 (1991).
- [68] S. Godfrey, Spectroscopy of  $B_c$  mesons in the relativized quark model, *Phys. Rev. D* **70**, 054017 (2004), arXiv:hep-ph/0406228 [hep-ph].
- [69] T. Barnes, S. Godfrey, and E. S. Swanson, Higher charmonia, *Phys. Rev. D* **72**, 054026 (2005), arXiv:hep-ph/0505002 [hep-ph].
- [70] S. Godfrey and K. Moats, Bottomonium mesons and strategies for their observation, *Phys. Rev. D* **92**, 054034 (2015), arXiv:1507.00024 [hep-ph].
- [71] S. Godfrey, K. Moats, and E. S. Swanson,  $B$  and  $B_s$  meson spectroscopy, *Phys. Rev. D* **94**, 054025 (2016), arXiv:1607.02169 [hep-ph].
- [72] S. Godfrey and K. Moats, Properties of excited charm and charm-strange mesons, *Phys. Rev. D* **93**, 034035 (2016), arXiv:1510.08305 [hep-ph].
- [73] S. Capstick and N. Isgur, Baryons in a relativized quark model with chromodynamics, *Phys. Rev. D* **34**, 2809 (1986).
- [74] Q.-F. Lü, Y. Dong, X. Liu, and T. Matsuki, Puzzle of the  $\Lambda_c$  Spectrum, *Nucl. Phys. Rev.* **35**, 1 (2018), arXiv:1610.09605 [hep-ph].
- [75] Q.-F. Lü, K.-L. Wang, L.-Y. Xiao, and X.-H. Zhong, Mass spectra and radiative transitions of doubly heavy baryons in a relativized quark model, *Phys. Rev. D* **96**, 114006 (2017), arXiv:1708.04468 [hep-ph].
- [76] G.-L. Yu, Z.-Y. Li, Z.-G. Wang, J. Lu, and M. Yan, Systematic analysis of single heavy baryons  $\Lambda_Q$ ,  $\Sigma_Q$  and  $\Omega_Q$ , *Nucl. Phys. B* **990**, 116183 (2023), arXiv:2206.08128 [hep-ph].

- [77] Z.-Y. Li, G.-L. Yu, Z.-G. Wang, J.-Z. Gu, and J. Lu, Systematic analysis of strange single heavy baryons  $\Xi_c$  and  $\Xi_b$ , *Chin. Phys. C* **47**, 7 (2023), arXiv:2207.04167 [hep-ph].
- [78] Z.-Y. Li, G.-L. Yu, Z.-G. Wang, J.-Z. Gu, and H.-T. Shen, Mass spectra of double-bottom baryons, *Mod. Phys. Lett. A* **38**, 2350052 (2023), arXiv:2210.13085 [hep-ph].
- [79] G.-L. Yu, Z.-Y. Li, Z.-G. Wang, J. Lu, and M. Yan, Systematic analysis of doubly charmed baryons  $\Xi_{cc}$  and  $\Omega_{cc}$ , *Eur. Phys. J. A* **59**, 126 (2023), arXiv:2211.00510 [hep-ph].
- [80] Z.-Y. Li, G.-L. Yu, Z.-G. Wang, J.-Z. Gu, and H.-T. Shen, Mass spectra of bottom-charm baryons, *Int. J. Mod. Phys. A* **38**, 2350095 (2023), arXiv:2211.15111 [hep-ph].
- [81] Z. Yang, G.-J. Wang, J.-J. Wu, M. Oka, and S.-L. Zhu, Novel Coupled Channel Framework Connecting the Quark Model and Lattice QCD for the Near-threshold  $D_s$  States, *Phys. Rev. Lett.* **128**, 112001 (2022), arXiv:2107.04860 [hep-ph].
- [82] Yu. S. Kalashnikova, Coupled-channel model for charmonium levels and an option for  $X(3872)$ , *Phys. Rev. D* **72**, 034010 (2005), arXiv:hep-ph/0506270 [hep-ph].
- [83] P. G. Ortega, J. Segovia, D. R. Entem, and F. Fernández, Coupled channel approach to the structure of the  $X(3872)$ , *Phys. Rev. D* **81**, 054023 (2010), arXiv:0907.3997 [hep-ph].
- [84] I. V. Danilkin and Yu. A. Simonov, Dynamical Origin and the Pole Structure of  $X(3872)$ , *Phys. Rev. Lett.* **105**, 102002 (2010), arXiv:1006.0211 [hep-ph].
- [85] M. Padmanath, C. B. Lang, and S. Prelovsek,  $X(3872)$  and  $Y(4140)$  using diquark-antidiquark operators with lattice QCD, *Phys. Rev. D* **92**, 034501 (2015), arXiv:1503.03257 [hep-lat].
- [86] S.-Q. Luo, B. Chen, Z.-W. Liu, and X. Liu, Resolving the low mass puzzle of  $\Lambda_c(2940)^+$ , *Eur. Phys. J. C* **80**, 301 (2020), arXiv:1910.14545 [hep-ph].
- [87] Z.-L. Zhang, Z.-W. Liu, S.-Q. Luo, F.-L. Wang, B. Wang, and H. Xu,  $\Lambda_c(2910)$  and  $\Lambda_c(2940)$  as conventional baryons dressed with the  $D^*N$  channel, *Phys. Rev. D* **107**, 034036 (2023), arXiv:2210.17188 [hep-ph].
- [88] B.-Q. Li, C. Meng, and K.-T. Chao, Coupled-channel and screening effects in charmonium spectrum, *Phys. Rev. D* **80**, 014012 (2009), arXiv:0904.4068 [hep-ph].
- [89] Q.-T. Song, D.-Y. Chen, X. Liu, and T. Matsuki, Charmed-strange mesons revisited: Mass spectra and strong decays, *Phys. Rev. D* **91**, 054031 (2015), arXiv:1501.03575 [hep-ph].
- [90] Q.-T. Song, D.-Y. Chen, X. Liu, and T. Matsuki, Higher radial and orbital excitations in the charmed meson family, *Phys. Rev. D* **92**, 074011 (2015), arXiv:1503.05728 [hep-ph].
- [91] C.-Q. Pang, J.-Z. Wang, X. Liu, and T. Matsuki, A systematic study of mass spectra and strong decay of strange mesons, *Eur. Phys. J. C* **77**, 861 (2017), arXiv:1705.03144 [hep-ph].
- [92] J.-Z. Wang, Z.-F. Sun, X. Liu, and T. Matsuki, Higher bottomonium zoo, *Eur. Phys. J. C* **78**, 915 (2018), arXiv:1802.04938 [hep-ph].
- [93] H. G. Dosch and V. F. Müller, Composite hadrons in non-Abelian lattice gauge theories, *Nucl. Phys. B* **116**, 470 (1976).
- [94] J. Carlson, J. Kogut, and V. R. Pandharipande, Quark model for baryons based on quantum chromodynamics, *Phys. Rev. D* **27**, 233 (1983).
- [95] R. Mizuk *et al.* (Belle Collaboration), Observation of an Isotriplet of Excited Charmed Baryons Decaying to  $\Lambda_c^+\pi$ , *Phys. Rev. Lett.* **94**, 122002 (2005), arXiv:hep-ex/0412069.
- [96] M. Artuso *et al.* (CLEO Collaboration), Observation of New States Decaying into  $\Lambda_c^+\pi^-\pi^+$ , *Phys. Rev. Lett.* **86**, 4479 (2001), arXiv:hep-ex/0010080.
- [97] K. Abe *et al.* (Belle Collaboration), Experimental Constraints on the Spin and Parity of the  $\Lambda_c(2880)^+$ , *Phys. Rev. Lett.* **98**, 262001 (2007), arXiv:hep-ex/0608043.
- [98] B. Aubert *et al.* (BABAR Collaboration), Observation of a Charmed Baryon Decaying to  $D^0p$  at a Mass Near  $2.94 \text{ GeV}/c^2$ , *Phys. Rev. Lett.* **98**, 012001 (2007), arXiv:hep-ex/0603052.
- [99] Z. Zhao, D.-D. Ye, and A. Zhang, Hadronic decay properties of newly observed  $\omega_c$  baryons, *Phys. Rev. D* **95**, 114024 (2017), arXiv:1704.02688 [hep-ph].